Analysis of multi-structured population models

by

Sabina Altus

B.S., University of Washington, 2011

M.S., University of Colorado Boulder, 2018

A thesis submitted to the

Faculty of the Graduate School of the

University of Colorado in partial fulfillment

of the requirements for the degree of

Doctor of Philosophy

Department of Applied Mathematics

2021

Committee Members:

David Bortz, Chair

Prof. Jeffrey Cameron

Prof. Nancy Rodriguez

Prof. Zachary Kilpatrick

Prof. Juan Restrepo

Altus, Sabina (Ph.D., Applied Mathematics)

Analysis of multi-structured population models

Thesis directed by Prof. David Bortz

Population dynamics are heavily influenced by the underlying structure or distribution of physiological features among individuals. Even when the governing dynamical system is linear, a population may converge to a stable structural distribution as it continues to grow exponentially in number. Asymptotic analysis provides a framework for establishing under what conditions this behavior can be expected in a cell population described by the linear, hyperbolic partial differential equation (PDE) model we have developed.

The motivation for developing this model was to better understand and characterize variation in photosynthetic capacity across growing microcolonies of cyanobacteria in an effort to support a broad range of industrial and agricultural applications. Cyanobacteria efficiently convert light energy into more stable forms of chemical energy, such as biomass, through a carbon concentrating mechanism. This process results in the formation of micro-compartments, called carboxysomes, which, once assembled, persist over many generations. As a result, wild-type cells contain both inherited carboxysomes, older than themselves, and more recently formed carboxysomes produced as they grow. Carboxysome productivity is a key factor driving cell growth, and is thought to decrease over time.

To investigate this claim, we have drawn from existing population models and expanded them to include an arbitrary number of structure variables, representing carboxysome ages in this application. Additionally, demographic parameters describing birth, death, and growth processes are age-, size-, and carboxysome-age-dependent. The evolutionary system is analyzed along with its associated linear operator and the strongly-continuous semigroup it is shown to generate. Two approaches to resolving the feedback mechanism of the reproductive process are discussed and shown to arrive at the same conclusion. The first approach is to

derive the family of step-response operators corresponding to reproduction viewed as a perturbation to the semigroup solution; and in the second, the renewal equation that emerges from the age $a = 0$ boundary condition is reduced to an eigenproblem. Both approaches ultimately allow us to characterize the asymptotic behavior of this population by decoupling evolution in time and state space.

Dedication

To my grandmother, Sabina, and to the survivors and defiant ones like her.

Acknowledgements

Thank you to my advisor, Prof. David Bortz, for your mentorship, patience, and unwavering support throughout this journey. I am sincerely grateful for all of the wisdom you've shared and the opportunities you've brought my way. I'd also like to thank our wonderful collaborator, Prof. Jeffrey Cameron, for making this project possible and for your guidance along the way. Thank you to Prof. Nancy Rodriguez, Prof. Zachary Kilpatrick, and Prof. Juan Restrepo for your encouragement, and all of the time and effort you have invested in me.

I would also like to express my gratitude to my parents, Kathryn and Joel Altus, and my brother, Gabriel Altus, for always believing in me and giving me the strength to take this on. A special thank you to my number one, Claire Bernhard, for being the greatest friend I could ask for.

A huge thank you to all of the Applied Mathematics faculty, staff, and my fellow graduate students at the University of Colorado, Boulder. I must give a special mention to Dr. Joy Mueller and Dr. Lewis Baker, friends and confidants without whom I would have been irretrievably lost. Finally, I'd like to recognize the women of the Association for Women in Math. Being a part of this organization has meant the world to me, and I am so happy to see it continue to grow and provide the support and encouragement that is so important to the success of all women in our field.

Contents

Chapter

Figures

Figure

Chapter 1

Introduction

1.1 Structured Population Modeling

Population structure refers to the way in which characteristics describing an individual are distributed across a population in aggregate. Structure has a decisive impact on population growth and survival, as death rates and reproductive behavior are contingent on physiological traits. Age-structured models form the foundation of structured population modeling, as age is generally the best descriptor of an individual's position in the life cycle. However, additional structure variables offer further insight into observed variations between individuals, even of the same age. This main contribution of the work presented in this dissertation is in extending existing structured population models to include an arbitrary number of structure variables, and showing that the traditional solution methods and population behavior they predict can similarly be adapted and reproduced in the larger multi-structured model.

In deriving continuously evolving structured population models, we consider the population as a distribution over its structure variables and impose conservation laws. The interpretation of a population as a distribution simply means that the size of the population at any time t is the integral of the distribution over all ages and structure variables. As such, structured population models consist of a balance law—a partial differential equation (PDE) describing population evolution in time, a boundary condition describing how new individuals enter the population, and an initial distribution. The first of this class of math-

ematical models was the linear age-structured model with age-specific birth and death rates proposed by Sharpe and Lotka in 1911 [58], and rederived by McKendrick in 1926 [48]. Since that time, this model has been generalized many times over to a size-structured model [59], an age-and-size-structured model [10, 11], as well as nonlinear versions of all of these [39, 47] (see G.F. Webb's monograph [67] on this topic for a more complete history).

In general, analysis of these structured equations has vastly expanded our understanding of how overall population dynamics are governed by the defining features of these classes (i.e., their fecundity and death rates) as well as the competitive or cooperative interactions between them, and their environment. These contributions have appeared in a wide variety of applications including epidemiology [35, 19], ecology [55], and cell biology [5], to name a few of the most pivotal examples.

A solution to a structured population model determines the population-level evolution as an aggregated picture of individual behavior as function of age or other structure variables. The general procedure for arriving at such a solution is by the method of characteristics. Applying the age $a = 0$ boundary condition describing births inevitably leads to a Volterra-type integral renewal equation at the boundary, solved by Laplace transform [12].

Extensions to age-structured models which include further structuring, and even nonlinear effects due to competition or crowding, continue to follow this central formulation and methodology [6]. The linear multi-structured model presented and analyzed in this dissertation similarly follows this general solution procedure, but in an abstract setting where solutions to the renewal equation are operators in a Banach space.

The motivation for developing the multi-structured model was to better understand how photosynthesis is regulated by structural components of varying efficiency within individual cyanobacterial cells. Mathematical modeling of population structure provides a framework for hypothesis testing and parameter estimation when model predictions are compared with data to evaluate a proposed relationship between certain structure variables to growth, death, and fecundity rates. Linear models are well suited for this purpose, as individual

behavior is fully determined by age and physiological state, and not in response to external factors, including the population as a whole. A linear model generally does not admit the possibility of reaching a steady-state solution, with the exception of a few special cases, e.g., the trivial zero solution. The long-term population-level behavior must be either reaching extinction or becoming infinitely large in infinite time. However, our asymptotic analysis will show that under certain conditions, a steady-state solution *in structure* is reached, while the population as a whole continues to grow without bound.

Asymptotic analysis is a broad field of study aimed at studying systems which require some resolution of processes occurring on small versus large scales. For many systems which, in general, do not converge to a steady-state, asymptotic analysis is the framework used to identify long-term behavior by separating the fast or short time processes with those unfolding over larger time scales [8]. For example, in a migrating or commuting population, the spatial distribution of individuals will reach equilibrium within a short amount of time, while population growth will continue indefinitely [44, 4]. Similarly, in a continuously evolving structured population, the distribution of individuals which can be grouped by physiological traits will stabilize within a short period of time, while again, population growth continues indefinitely.

The evolution equations describing demographic processes, e.g., birth, death, and growth, are viewed abstractly as an operator $\mathcal{A}$ acting on a Banach space $\mathcal{B}$, which is shown to generate a strongly-continuous semigroup $S(t)$ of linear operators mapping $\mathcal{B}$ into itself. The semigroup approach is particularly advantageous for modeling cell populations as they allow for 'jumps' in the state space, that is, when a cell divides it may disappear from the population and reappear in a different form at the age $a = 0$ boundary—not a possibility for classical solutions to a PDE. Spectral properties of the operator $\mathcal{A}$, specifically the dominant eigenvalue λ_0 and corresponding eigenvector (or eigenfunction) ψ_{λ_0}, provide a decomposition of the solution space $\mathcal{X} = \mathbb{R}_+ \times \mathcal{B}$ into two invariant subspaces: the eigenspace spanned by the eigenvector corresponding to the dominant eigenvalue, $\mathcal{X}_{\lambda_0}$, and its comple-

ment $\mathcal{X}_{\lambda_0}^c = \mathcal{X} \setminus \mathcal{X}_{\lambda_0}$. Under this decomposition, we find that, as $t \to \infty$ the semigroup acting on elements from the complement space go to zero, while the semigroup acting on the eigenspace grows exponentially [47]. Let $\phi \in \mathcal{X} = \psi_{\lambda_0} + \psi^c$, where $\psi_{\lambda_0} \in \mathcal{X}_{\lambda_0}$, and $\phi^c \in \mathcal{X}_{\lambda_0}^c$, then

$$\lim_{t\to\infty} S(t)\phi = \lim_{t\to\infty} \left(S(t)\psi_{\lambda_0} + S(t)\psi^c\right) = e^{\lambda_0 t}\psi_{\lambda_0}.$$

In this way, the asymptotic behavior of the system can be characterized as the long time behavior of the semigroup acting to advance in time the stable structural distribution of the population, reached after a short transient phase.

Discrete time analogous example For completeness, here we present an introductory example of structured population modeling in a discrete setting[1] . The solution and its decomposition into separate time and age dependent parts is entirely analogous to the solution in the continuous setting. These abstract concepts can be made concrete in the discrete setting. We form an age-structured model by dividing our population into N discrete age classes and evolve the distribution at time t, $\mathbf{n}_t \in \mathbb{R}^N$, forward by multiplying by a Leslie matrix $\mathbf{L}$, the discrete-time analogue of a system of evolution equations. For example, if $N = 4$, our Leslie matrix system might look like,

$$\mathbf{n}_{t+1} = \begin{bmatrix} P_1 & 0 & F_3 & F_4 \\ G_1 & P_2 & 0 & 0 \\ 0 & G_2 & P_3 & 0 \\ 0 & 0 & G_3 & P_4 \end{bmatrix} \mathbf{n}_t = \mathbf{L}\mathbf{n}_t = \mathbf{L}^t\mathbf{n}_0 \tag{1.1}$$

where P_i represents the probability that an individual survives, but remains in the same age class, G_i represents the probability that an individual survives and advances to the next age class, and F_i is the fecundity rate for that age class. Since all of these vital rates are required to be positive, the Perron-Frobenius Theorem guarantees a positive largest eigenvalue, λ_0, and corresponding positive eigenvector ψ_{λ_0}. Let $\mathcal{A} = \mathbf{L}^t$ be our evolution operator, then the

[1] For those with prior training in mathematical biology, this section may be skipped.

semigroup $S(t) = e^{\mathcal{A}}$, the matrix exponential. Writing $\mathbf{n}_0$ as a linear combination of the eigenvectors of $\mathbf{L}$, we find that,

$$\begin{aligned}
\mathbf{n}_{t+1} &= c_0\mathcal{A}\psi_{\lambda_0} + c_1\mathcal{A}\psi_{\lambda_1} + c_2\mathcal{A}\psi_{\lambda_2} + c_3\mathcal{A}\psi_{\lambda_3} \\
&= c_0\lambda_0^t\psi_{\lambda_0} + c_1\lambda_1^t\psi_{\lambda_1} + c_2\lambda_2^t\psi_{\lambda_2} + c_3\lambda_3^t\psi_{\lambda_3} \\
\lim_{t\to\infty} \mathbf{n}_{t+1} &= \lim_{t\to\infty} c_0\lambda_0^t \left(\psi_{\lambda_0} + c_1 \left(\frac{\lambda_1}{\lambda_0}\right)^t \psi_{\lambda_1} + c_2 \left(\frac{\lambda_2}{\lambda_0}\right)^t \psi_{\lambda_2} + c_3 \left(\frac{\lambda_1}{\lambda_0}\right)^t \psi_{\lambda_3} \right) \\
&= c_0\lambda_0^t\psi_{\lambda_0} \\
&= c_0 e^{\lambda_0 t}\psi_{\lambda_0}
\end{aligned}$$

In this example, we have shown that the long-term behavior of a structured population is determined by the spectral properties of its evolution operator. The population age-structure reaches a steady state determined by the dominant eigenvector of the evolution operator, while the population continues to grow exponentially at the rate given by the dominant eigenvalue.

1.2 Outline

In this dissertation, we present a multi-structured partial differential equation model of a cyanobacteria population. This model extends existing age and size structured models to include an arbitrary, finite number of additional structure variables. The central advancement achieved by the analysis presented in this dissertation is to demonstrate that the methods used to solve and predict the asymptotic behavior of existing age-, or age-and-size structured models of cell populations can be applied successfully to the multi-structured model, and similarly resolve the asymptotic behavior into a time-dependent operator acting on a stable-structural distribution in an invariant subspace of the state space.

In Chapter 2, we present the biological motivation for the development of this model, as well as a biomechanical model for the very early (on the order of 1 to 32-cell) stages of a growing cyanobacterial microcolony. While the multi-structured model that is the focus of

this dissertation is not concerned with colony development at the early stages, this section includes our first contributions to understanding this problem and the work presented here was included in two publications [49, 41]. The biomechanical model described in this chapter identifies points of contact between cells where a repulsive force is applied. At these contact points, light is emitted rather than absorbed due to the cell regulating its growth in response to mechanical stress. Model generated simulations are shown to be in agreement with time-lapse fluorescence microscopy images.

In Chapter 3, the multi-structured model is presented and solved using the method of characteristics. A series solution is presented for the integral renewal equation derived at the age $a = 0$ boundary. While we prove that a continuous solution exists, it is not possible to express such a solution in a closed form. The next two chapters present two different approaches to reach an asymptotic solution for the long-term behavior of this population.

Chapter 4 introduces semigroup theory and the beneficial properties of a semigroup solution. We provide some of the key theorems and results of this rich theoretical framework before applying them to the multi-structured model and showing that the model solution of the previous chapter is a semigroup of linear operators. To resolve the boundary condition describing cell renewal, we consider a perturbation to the generator of the semigroup solution, and determine the long-term behavior of the perturbed semigroup it generates by analysis of the spectral properties of the perturbed generator. This connection is made by defining a step-response operator describing how the system responds to an input entering at the age $a = 0$ boundary. Convolution of the step-response with the original semigroup becomes the perturbation (to the orignial semigroup) through which the perturbed semigroup is defined. Taking Laplace transforms of the equations relating the semigroups leads to a characteristic equation for the dominant eigenvalue of the perturbed generator, and we show that this eigenvalue and its corresponding eigenfunction determine the asymptotic behavior of the system. We conclude this chapter by deriving and explicitly stating this eigenproblem.

In Chapter 5, we derive a similar eigenproblem beginning from the renewal equation

at the age $a = 0$ boundary cast as an abstract renewal equation of operators in a Banach space. Applying Laplace transforms to the abstract equation allows us to reduce it to an eigenproblem as the long-term behavior of the system is determined by singularities of the convolution operator appearing in the renewal equation. We show that this singularity is uniquely determined by the eigenvalue for which the spectral radius of this operator is equal to one, and again conclude the chapter by deriving and explicitly stating this eigenproblem.

Solving the eigenproblem requires specification of conditions for cell division. In Chapter 6 we solve the eigenproblem under a set of such conditions and discuss the resulting solutions and their interpretation. Finally, we conclude with a discussion of our analysis and results including future applications and amendments to the multi-structured model.

Chapter 2

Cyanobacteria

This chapter details the biological motivation for studying cyanobacteria and the advantage this brings to many important applications. The biomechanical model presented in the second section of this chapter has a separate focus from the multi-structured model presented in the next chapter. However, the biomechanical model was a successful contribution to first grappling with the problem of understanding photosynthesis in cyanobacteria. The results presented here were published in *Nature microbiology* [49], and included as part of a followup published in *Science advances* [41].

2.1 Biological Motivation

Cyanobacteria play a critical role in the global carbon cycle. Prehistorically, they are credited with oxygenating the earth's atmosphere, and they continue to perform over 35% of global carbon fixation, despite comprising less than 0.2% of all photosynthetic biomass [57, 7]. In order to maintain their efficiency in today's ambient CO_2 levels (low from their point of view), cyanobacteria have evolved a carbon concentrating mechanism (*ccm*) which encapsulates the necessary enzymes for carbon fixation into microcompartments called *carboxysomes*. Specifically, a carboxysome is an icosahedral protein shell containing the key enzymes ribulose 1, 5-biphosphate carboxylase/oxygenase (RuBisCO) and carbonic anhydrase. The carboxysome's role in carbon fixation is depicted in Figure 2.1 where two molecules of 3-phosphoglycerate, an antecedant of the sugars and amino acids the cell uses as an energy

source or to form biomass, are produced from a single carbon-containing molecule. Concentrating the enzymes in this way boosts their catalytic efficiency as CO_2 is aggregated so as to maximize contact with these enzymes at a distance from oxygen, a competing substrate [17]. The vital operation of carbon fixation as the gateway to all other metabolic processes in the cell illustrates the dependency of cell growth upon carboxysome efficacy.

Carboxysomes are the dominant contribution in regulating growth at both the cellular and population level, and the model presented in this work aims to elucidate this mechanism. This will bring valuable insight to advance large-scale industrial applications in clean energy, such as carbon sequestration, and the production of biofuels or bioplastics derived from the hydrocarbon chains forming the cell membrane [46], as well as more recently proposed agricultural applications exploring the possibility of boosting yield by transferring carboxysomes to plants, thus increasing their photosynthetic capability [37].

The assembly pathway of a carboxysome is well understood [17]; however, detailing the life-cycle of a carboxysome is an active area of research. In recent years, fluorescence-microscopy imaging has been used more broadly and this powerful technology has allowed our collaborators in the Cameron Lab at RASEI, the Renewable and Sustainable Energy Institute, to develop a platform to measure carboxysome number, position, and activity over time in a growing cyanobacteria population [41]. One class of these experiments is focused on measuring the contribution of a single carboxysome. This is performed by knocking out the *ccm* operon, the collection of genes encoding for the formation of new carboxysomes, so that after a few generations, many cells contain only a single carboxysome. For a cell with a single carboxysome (at ambient CO_2), all carbon fixation, and therefore growth, can be attributed to the catalytic activity of that carboxysome [41]. Therefore, we may use the growth rate of the cell as a measure of carboxysome activity over time.

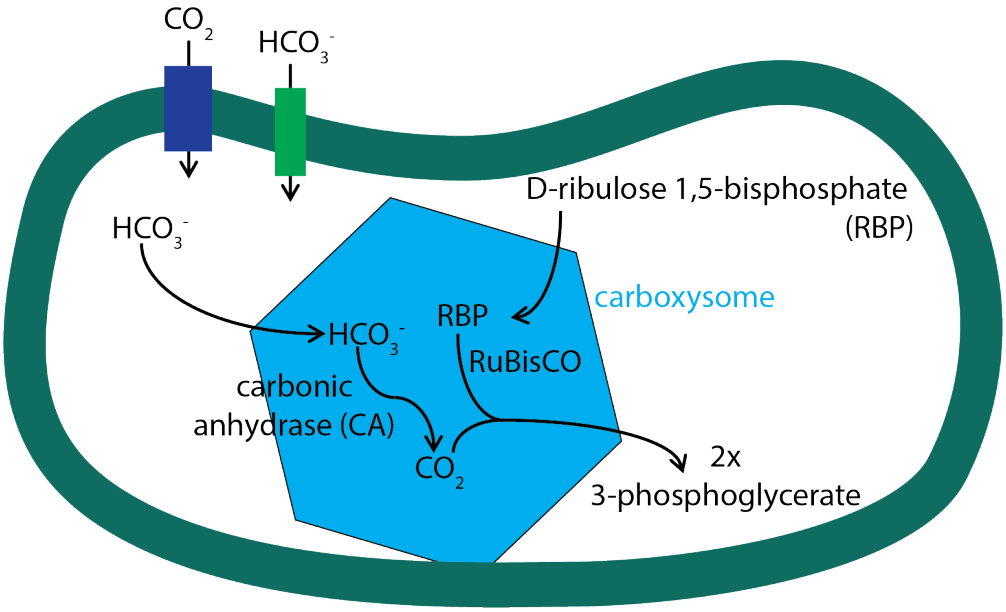

Figure 2.1: An illustration of the carbon concentrating function of a carboxysome within a cyanobacterial cell, and the key enzymes involved in this process. Bicarbonate (HCO_3^-) enters the cell and is shuttled into the carboxysome where carbonic anhydrase catalyzes the reversible reaction transforming bicarbonate into CO_2 and water. Each carbon dioxide molecule then reacts with RuBisCO to form two 3-phosphoglycerate molecules, required to produce biomass and usable energy for the cell [53]. Image from [14]

.

2.2 Preliminary investigation

Prior to developing the multi-structured model, we wanted to better understand the growth dynamics of this population, including additional factors that impact photosynthetic capability at every stage of microcolony growth. To that end, we began with a biomechanical model of early-stage microcolony development. For completeness, here we present the biomechanical model.

2.2.1 Force of cell-cell interactions

Photosynthesis is regulated by individual cells in response to their environment. Improving efficiency at the larger, micro-colony scale requires a full biomechanical picture of cell-to-colony dynamics. Colonies grown under a substrate with no boundary constraint are observed to self-organize spatially. Patterns observed repeatedly at the 4-, 8-, 16-, and 32-cell stages eventually grow into round colonies comprised of regions of cells all oriented in the same direction. The shape and structure of the resulting colony are principally guided by the competition between steric, repulsive forces between neighboring cells as they push each other out of the way and, the extensile stress a cell experiences as it attempts to grow in a confined area. These forces govern micro-colony morphology at the early stages of growth and have a large impact on the resulting behavior and characteristics of the colony as it expands to become a biofilm.

2.2.2 Biomechanical model

Biofilms typically grow from a single bacterial cell elongating and dividing to form a highly organized and repeatedly observed spatial structure at the early microcolony stage. Self-organization is primarily the result of steric, repulsive forces that tend to order the colony as neighboring cells push each other out of the way and into alignment with one another. In this way, colonies may aggregate into nematic micro-domains reminiscent of those seen

Figure 2.2: Time-lapse images of a growing cyanobacterial microcolony. The darker purple to red regions indicate where light is being absorbed by the cell, whereas bright orange to yellow regions indicate little to no light absorption. Interior-colony cells experience the most mechanical stress and regulate their growth by slowing photosynthesis in response. The pronounced W-shape appearing at the 8-cell stage condenses to align cells in the interior of the colony, as seen at the 16-cell stage in the right-most image. Images from [49]

.

in active liquid crystals [36]. However, steric forces must balance with extensile stress which brings disorder to the colony as cells struggle to grow in a confined area. Competition between these two forces can disrupt the balance between them, fracturing nematic regions or even bring about a transition from mono-layer to multi-layer growth [60]. However, these later-stage phenomena will not be reported on here, as the focus of the biomechanical model is in simulating the organization and asymmetry observed at the earliest stages of microcolony formation from a single cell.

A biomechanical model of microcolony formation in cyanobacteria is presented to investigate and support the claim that cyanobacteria regulate photosynthesis in response to mechanical stress. As described above, the primary mechanical forces considered are steric forces from cell-cell interactions and extensile stress from friction and crowding. Of particular interest is the way in which these forces effect the photosynthetic capability of an individual cell and the impact on the colony as a whole. Cells under mechanical stress do not have space to grow freely, and therefore, become limited in the amount of light they can absorb. The excess light is then reflected away from the cell causing them to appear brightly in fluorescence microscopy images, as depicted in Figure 2.2. As a result, cell growth in the densely packed interior of the colony is expected to be slower than for those cells at the periphery, and experimental data is in agreement with this assumption.

Cell colonies occupy a two-dimensional space with no boundary constraint. Throughout the simulation, cells maintain a constant width, and grow only along their major body axis. Cell division is symmetric in that the mass of a dividing cell is split evenly to form two daughter cells, and a cell divides upon reaching the division length L_{div}. Crucially, cyanobacteria are observed to bend in a prescribed way as they divide. To replicate this observed behavior in simulation, the angle between the major body axis of two recently divided cells is just under 180 degrees, rather than in perfect alignment.

The main loop of the model consists of two parts which can be regarded as a *bio*-part describing individual growth and division, and a *mechanical*-part describing how cells interact with one-another. First, cell length increases according to an ODE exponential growth model. Cells which have reached the division length are then replaced by two daughter cells of equal length. In reality, cell division does not occur instantaneously, so to mimic the slow process of septum formation preceding the full separation of the two daughter cells, a spring-like attachment exists temporarily between recently divided cells with a strength k_s which falls off linearly in time until it reaches zero, at which time the connection is deleted. The second part of the loop adjusts cell position and orientation in response to cell-cell interactions and frictional forces according to Newtonian mechanics, that is, by computing the net force acting on each cell and integrating the resulting acceleration to find its new position.

The remaining sections of this chapter give the model equations and specifications, and conclude with a comparison of our simulation results with time-lapse fluorescence images of a growing microcolony captured in vivo. The structure and governing equations of this model are largely adapted from [60] and [36].

2.2.3 Cell Properties and Growth

Each cell is modeled as a sphero-cylinder of fixed radius, $r = 1$, and variable length, L, referring to the body axis of the cell, as illustrated in Figure 2.3. At each time step, cell

length is increased according to the exponential growth model, $\frac{dL}{dt} = \alpha L$. Division occurs once cell length reaches or exceeds 2.5 times its radius. Following cell growth and division, the force of friction between the cell wall and the agar on which it is grown, and the force of cell-cell interaction exerted on each cell by its neighbors, are calculated and applied as updates to cell position and orientation by integrating numerically[1] the system of equations derived from Newtonian mechanics [60].

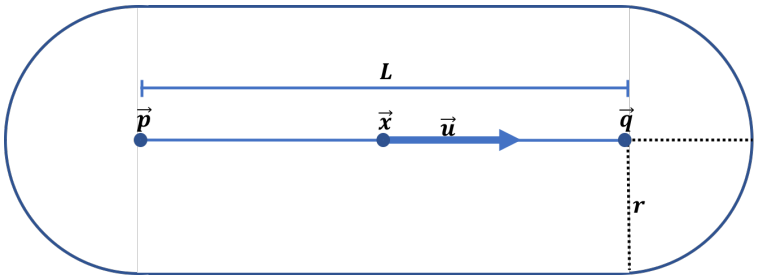

Figure 2.3: Sphero-cylinder model of a cyanobacterial cell. The position of the i^{th} cell $(i = 1, 2, ...)$ is given by its center of mass, $\mathbf{x}_i$. The orientation of a cell, $\mathbf{u}_i$, is given as a unit vector pointing along the major axis of the cell such that if a cell were positioned at the origin, $\mathbf{u}_i$ would point in the direction of the positive x-axis. The length of the cell, also referred to as its body axis, is the line segment joining the points $\mathbf{p}_i$ and $\mathbf{q}_i$. The width of each cell is then equal to $2r$, and remains constant for all time for all cells.

Cell mass and moment of inertia are functions of cell length and radius, and are similarly adjusted at each time step. Without loss of generality, we will adopt the biologically reasonable assumption that cell density ρ is equal to 1, the density of water [60]. Let m_i be the mass of the i^{th} sphero-cylindrical cell, then

$$m_i = \rho\left[\frac{4}{3}\pi r^3 + \pi r^2 L\right],$$

and its moment of inertia I_i is,

$$I_i = \frac{1}{48}\pi\rho(2r)^2L^3 + \frac{3}{64}\pi\rho(2r)^4L + \frac{1}{60}\pi\rho(2r)^5 + \frac{1}{24}\pi\rho 2r^3L^2.$$

Initially, each cell grows at the average rate, α_{avg}, taken to be 0.224 $\frac{\mu m}{s}$, for an average doubling time of just over three hours. However, decreased photosynthetic activity for cells

[1] Both the growth model and equations of motion are integrating using MATLAB's built-in ODE solver *ode45*.

in the tightly packed colony interior leads to a slow-down in growth. The growth rate, α, then decreases linearly to a minimum of 0.218 as the total force acting on a particular cell increases.

2.2.4 Cell Division

Reproducing the repeatedly observed W-shape most clearly seen in the 4- and 8-cell stages, requires two adjustments which serve to model cell division more accurately as a process, rather than an instantaneous event. That is, according to the model, a cell splits instantaneously to form two daughter upon reaching the division length. However, in reality, cell division occurs through continuous deformation of the cell wall forming a septum between daughter cells before they fully separate. During this process, one daughter cell will generally grow slightly faster than its sister, depending on its position in the colony, and begin to push her out of the way and bringing them out of alignment. Therefore, the first adjustment included in our model is a perturbation to cell orientation following division by an angle $\theta \in [\pm 1^\circ, \pm 10^\circ]$ according to cell position.

Secondly, an ephemeral connection is maintained between recently divided cells, modeled as a spring, the stiffness of which, k_s, falls off linearly in time from its initial value k_0 until it is deleted after a period of time t_*. The spring "constant" k_s is then a function of the length of time since division t_{sd} given by

$$k_s(t_{sd}) = \begin{cases} k_0(1 - t_{sd}/t_*), & \text{for } t_{sd} < t_* \\ 0, & \text{for } t_{sd} \geq t_*. \end{cases}$$

2.2.5 Mechanics

Let the two-dimensional vector $\mathbf{F}_i$ be the net force acting on the i^{th} cell with vector components giving the net force in the $x-$ and $y-$directions, respectively. Then,

$$\mathbf{F}_i = \mathbf{F}_{cs} + \sum_{j \neq i} \mathbf{F}_{ij}.$$

The first term, $\mathbf{F}_{cs}$, represents the force of friction acting on cell i by contact with the surrounding substrate, and the sum accounts for cell-cell interactions, where each term $\mathbf{F}_{ij}$ denotes the elastic, repulsive force cell j exerts on cell i. Note that $\mathbf{F}_{ii} = 0$, and $\mathbf{F}_{ij} = \mathbf{F}_{ji}$.

The mechanical system within the model is governed by the following three equations describing the spatial translation of the i^{th} cell in response to the mechanical forces acting upon it,

$$\begin{aligned} m_i \frac{d^2\mathbf{x}_i}{dt^2} &= \mathbf{F}_i \\ I_i \frac{d\omega_i}{dt} &= \tau_i \\ \frac{d\mathbf{u}_i}{dt} &= \omega_i \times \mathbf{u}_i \end{aligned} \tag{2.1}$$

where τ_i is the net torque acting on cell i, and ω_i is its angular velocity.

2.2.6 Cell-Cell Interactions

The force exerted on cell i by cell j is calculated from the formula,

$$\mathbf{F}_{ij} = k\Delta_{ij}\hat{\mathbf{n}}_{ij} \tag{2.2}$$

where $\hat{\mathbf{n}}_{ij}$ is a unit vector indicating the direction along which the force is applied, Δ_{ij} is the degree of deformation which, if nonzero, signifies a repulsive interaction occurring between the i^{th} and j^{th} cells, and finally, the constant k gives the strength of cell-cell interactions, a measure of cell stiffness[2] .

To determine the force direction $\hat{\mathbf{n}}_{ij}$ and resulting degree of deformation, Δ_{ij}, cells are allowed to 'overlap,' theoretically, and we calculate the shortest distance s between their body axes [36]. The degree of overlap or deformation Δ_{ij} is zero, when $2r < s$, in which case the distance between the i^{th} and j^{th} cells is great enough that they are not in contact (recall

[2] Formally, k is determined by the Young's modulus of the cell, a measure of the stress (force per unit area) required to deform the cell by a given amount. However, without access to the Young's modulus of this particular strain, the value used in model simulations was approximated from values reported in the literature for *E. coli* [36].

that r is the cell radius) and $\mathbf{F}_{ij}$ vanishes, and nonzero if $2r > s$ suggesting that these cells do 'overlap' and therefore exert a force on one another. When Δ_{ij} is nonzero, it takes on the value $2r - s$, the distance over which the repulsive force is applied, and the two closest points along the body axis of the i^{th} and j^{th} cells, $\mathbf{t}_i$ and $\mathbf{t}_j$, respectively, become the contact points for this interaction.

The normalized vector from contact point $\mathbf{t}_j$ to $\mathbf{t}_i$,

$$\hat{\mathbf{n}}_{ij} = \frac{\mathbf{t}_i - \mathbf{t}_j}{|\mathbf{t}_i - \mathbf{t}_j|}. \tag{2.3}$$

determines the direction along which the repulsive force $\mathbf{F}_{ij}$ is applied to the i^{th} cell. If cells are nearly parallel, such that contact points cannot be uniquely identified, the center of mass is used as the contact point, as in, $\mathbf{t}_i = \mathbf{x}_i$ and $\mathbf{t}_j = \mathbf{x}_j$.

The three two-cell configurations in Figure 2.4 depict the three possible scenarios in which an elastic cell-cell interaction may occur. Cells are shown to overlap in this illustration to convey how $\mathbf{F}_{ij}$ is derived as a force of strength k applied in the direction $\hat{\mathbf{n}}_{ij}$ over a distance Δ_{ij}, the length of the line segment s falling within the overlapping region. The force $\mathbf{F}_{ij}$ exerted by cell j acts to push cell i out of its way, and equivalently for $\mathbf{F}_{ji}$, and as a result, no overlapping cells appear in model simulations, as expected.

2.2.7 Frictional Forces

Friction between cells and the substrate (agar gel pads), is proportional to the velocity, $\mathbf{v}$, or angular velocity, ω_i, of the cell with respect to the agar. Friction inhibiting translational motion is given by,

$$\mathbf{F}_{cs} = -b_t \mathbf{v} \tag{2.4}$$

where b_t is the friction coefficient for translation.

The i^{th} cell experiences a net torque given by,

$$\tau_i = (\mathbf{t}_i - \mathbf{x}_i) \times \mathbf{F}_{ij} - b_r \omega_i \tag{2.5}$$

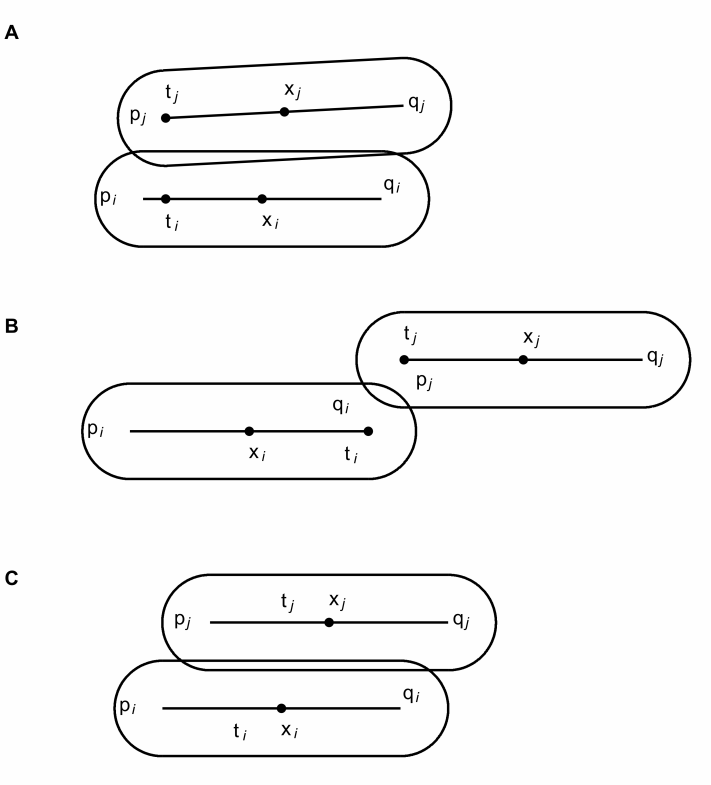

Figure 2.4: Depicted here are the three possible ways that two cells may interact by exerting a force on one another. The first (A) is by contact at a distinct point along the body axis, the second (B) is by end-to-end contact, and the third (C) is when two nearly parallel cells come in contact and the unique point of contact cannot be identified. The places where cells overlap illustrate the interpretation of Δ_{ij} as the distance over which the force of cell-cell interaction is applied. Image from [60].

where b_r is the friction coefficient for rotation[3] . The point $\mathbf{t}_i$ appearing in (2.5) is the same contact point inside cell i where the force from cell j is most directly applied.

2.2.8 Numerical implementation

The linear system (2.6) fully describes the mechanical component of the biomechanical model. At each time step, the system is solved for each cell and its position and orientation are updated accordingly. Velocity and angular velocity are also updated and become the initial conditions for the next iteration. Superscripts such as $\mathbf{x}^{(N)}$, denote the N^{th} component of the corresponding vector. Note that the orientation vector $\mathbf{u}$ is appended to include a zero as its z-component.

$$\frac{d}{dt}\begin{bmatrix} \mathbf{x}^{(1)} \\ \mathbf{x}^{(2)} \\ \mathbf{v}^{(1)} \\ \mathbf{v}^{(2)} \\ \omega^{(1)} \\ \omega^{(2)} \\ \omega^{(3)} \\ \mathbf{u}^{(1)} \\ \mathbf{u}^{(2)} \\ \mathbf{u}^{(3)} \end{bmatrix}_i = \begin{bmatrix} \mathbf{v}^{(1)} \\ \mathbf{v}^{(2)} \\ (1/m)[(\sum \mathbf{F}_{ij})^{(1)} - b_t\mathbf{v}^{(1)}] \\ (1/m)[(\sum \mathbf{F}_{ij})^{(2)} - b_t\mathbf{v}^{(2)}] \\ (1/I)((\sum(\mathbf{t}_i - \mathbf{x}_i) \times \mathbf{F}_{ij})^{(1)} - b_r\omega^{(1)}) \\ (1/I)((\sum(\mathbf{t}_i - \mathbf{x}_i) \times \mathbf{F}_{ij})^{(2)} - b_r\omega^{(2)}) \\ (1/I)((\sum(\mathbf{t}_i - \mathbf{x}_i) \times \mathbf{F}_{ij})^{(3)} - b_r\omega^{(3)}) \\ \omega^{(1)} \times \mathbf{u}^{(1)} \\ \omega^{(2)} \times \mathbf{u}^{(2)} \\ \omega^{(3)} \times \mathbf{u}^{(3)} \end{bmatrix}_i \tag{2.6}$$

[3] The true force of friction between these cells and their agar substrate is, as of yet, unknown. Instead, both coefficients were chosen to most accurately match experimental observations, i.e., small enough so as not to interfere with cell growth and to allow for movement, but large enough that cells at the periphery of the colony do not slide or spin away from the colony when pushed by another cell. The frictional coefficients for the model presented in [60] were similarly determined, a method the authors describe as, "by trial and error."

2.3 Results and Conclusion

We conclude this chapter by presenting in Figure 2.5 a comparison of time-lapse fluorescence images of a growing microcolony against still images taken from simulations of the biomechanical model we developed. Simulated cells are colored according to the net force acting upon them, cells under the least amount of mechanical stress appear in purple, increasing to red, then orange, and finally, yellow for the highest amount of mechanical stress. Points on the cell wall where a force is being applied are lit up in white, fading to black according to the magnitude of the applied force. The biomechanical model replicates colony morphology through the 16-cell stage, and moreover, there is good agreement between the position of simulated cells under the various levels of mechanical stress and the brightness of corresponding cells in the fluorescence images.

The biomechanical model we have developed is able to accurately match the observed morphology and spatial distribution of mechanical force within a growing cyanobacterial microcolony, under the assumption that cells under mechanical stress grow more slowly. This result supports the claim published in [49] asserting that cyanobacteria regulate their photosynthetic activity, which has the direct effect of slowing cell growth, in response to mechanical stress.

Furthermore, the repeatedly observed folding pattern (beginning at the 4-cell stage) leading to cell alignment in the colony interior, appears in a similar manner in other cyanobacterial strains—including, for example, the filamentous nitrogen-fixing *Anabaena*. Future work will include adapting this model to replicate and characterize colony morphology for an array of cyanobacterial strains. Here we have presented a model wherein colony morphology emerges as the result of cells simply obeying Newtonian mechanics, and [less simply] regulating their growth in response to mechanical stress as they compete for space to grow and divide. The central goal of this work moving forward is then to classify expected or observed colony morphologies by asymmetries in cell growth emerging at the earliest stages

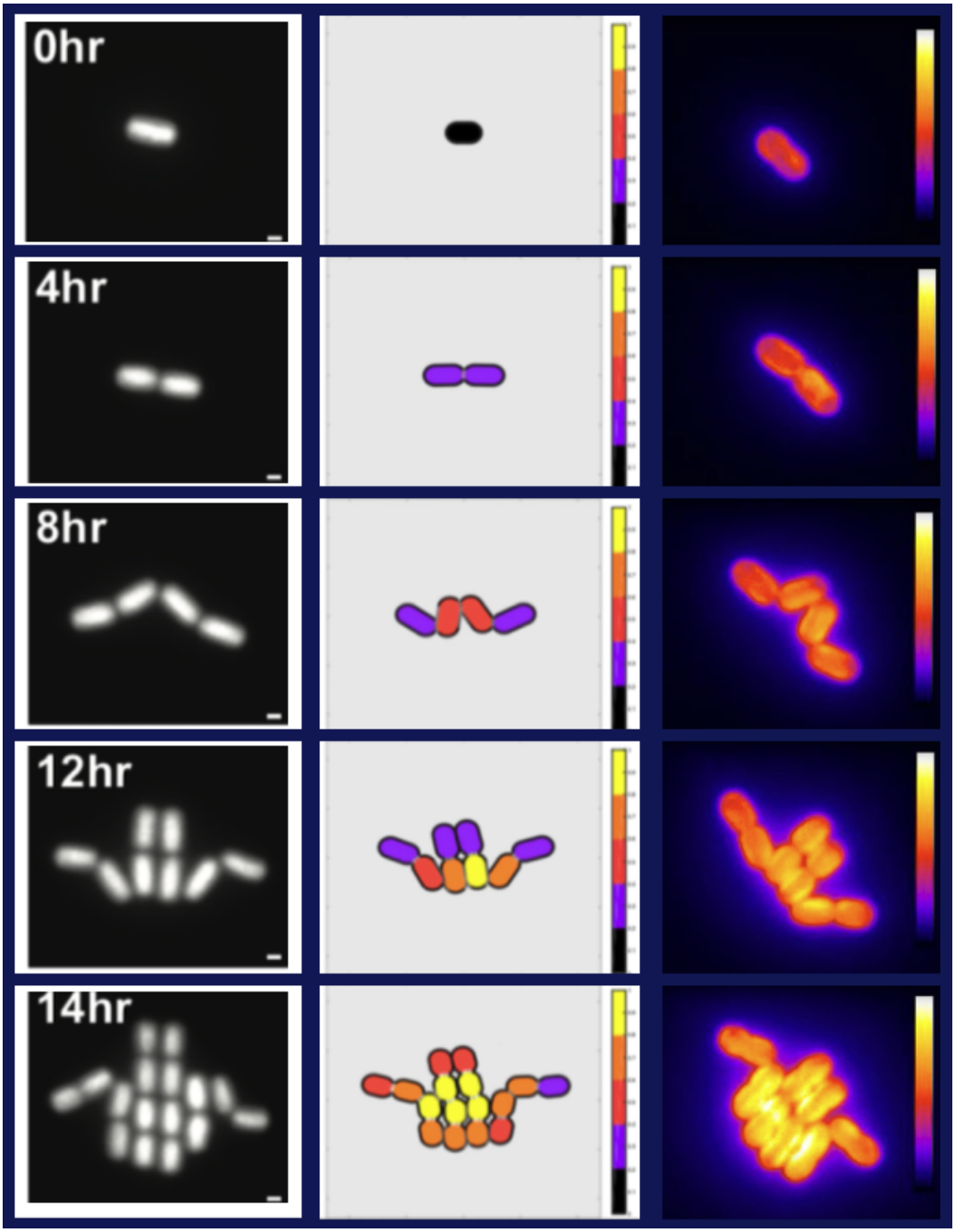

Figure 2.5: A comparison of model simulated cell growth with data. The black and white images at left depict the emergence of the aforementioned repeatedly observed early-stage colony morphology, the middle images are taken from model simulations, and the images at right show an increase in cell fluorescence as the colony grows and more cells compete for space. In the simulation images, the location where a force is applied to the cell surface is lit up in white. Cells under the greatest amount of mechanical stress are in yellow, then orange, then red, and finally purple for cells experiencing little to no external force.

of colony formation.

Chapter 3

Multi-structured Modeling

3.1 The multi-structured model

The multi-structured model presented in this chapter and its analysis are the focus of the remainder of this dissertation. The partial differential equation-based model we present was developed to evaluate the claim that carboxysome efficacy decreases over time. To that end, the state of an individual cell is characterized by its age, length, and k additional structure variables each representing the age of one of its carboxysomes. Including the additional structure variables and expanding to a multi-structured model is required to describe the evolution of this population, because cyanobacteria naturally contain carboxysomes of different ages. Once these microstructures are formed, they remain intact, even through cell division. Furthermore, carboxysomes take up space inside the cell, and so the formation of new carboxysomes is necessarily concurrent with growth, as opposed to all at once. A typical cell will have both inherited carboxysomes older than itself, as well as the carboxysomes it has formed since birth. The multi-structured model then, using carboxysome age as a proxy for efficacy, is needed in order to capture the dynamics of this population and identify the true relationship between carboxysome age and efficacy.

In this chapter, the model is presented and solved using the method of characteristics. The solution in the region where age is greater than time is fully determined by propagating the initial distribution forward in time. However, incorporating the boundary condition at the age $a = 0$ boundary leads to a renewal equation which does not admit a closed form

solution. A power series representation of the solution to the renewal equation is given, and used to prove the existence and uniqueness of a continuous solution. In light of this result, we conclude this chapter by introducing two approaches to finding an asymptotic solution.

3.1.1 Model components

The motivation for developing this model is most clearly described through the growth curves and cell length at birth data seen in Figure 3.1. As we have seen, carbon fixation is performed inside the carboxysome and this is the first, crucial step in cyanobacterial metabolism. By interrupting protein expression within the *carbon-concentrating-mechanism*-operon, the formation of new carboxysomes is effectively turned off, and after a few cell cycles, many cells will contain only a single carboxysome [17]. With a single carboxysome, all of the growth of that cell and its future lineage can be attributed to that one carboxysome. Part (A) of Figure 3.1 depicts cell length over time for a chosen cell lineage. Carboxysome formation is turned off at time zero, and the green curves at left show length over time for the originator of this lineage, and her daughter and granddaughter, all grown with more than one carboxysome. The curves to right of the vertical dashed line in blue show cell length over time for the last three generations of this lineage, all of which were grown by one carboxysome. Clearly, the blue curves show a decrease in both the growth rate and length at birth, as this carboxysome is passed from one generation to the next. The data plotted at right in part (B) corroborates this story as each pink dot represents the length at birth of a cell containing a single carboxysome, and the vertical bars separate generations. The mathematical model presented here builds on the hypothesis that carboxysome functionality decreases over time, and we intend to use this model as a framework for understanding the rate at which degradation occurs and in what way this dictates overall population dynamics.

In order to investigate how carboxysome efficacy governs population dynamics in cyanobacteria, we will need to resolve the *structure* of the population. As opposed to aggregate models such as, the linear Malthusian or nonlinear Logistic growth models, wherein

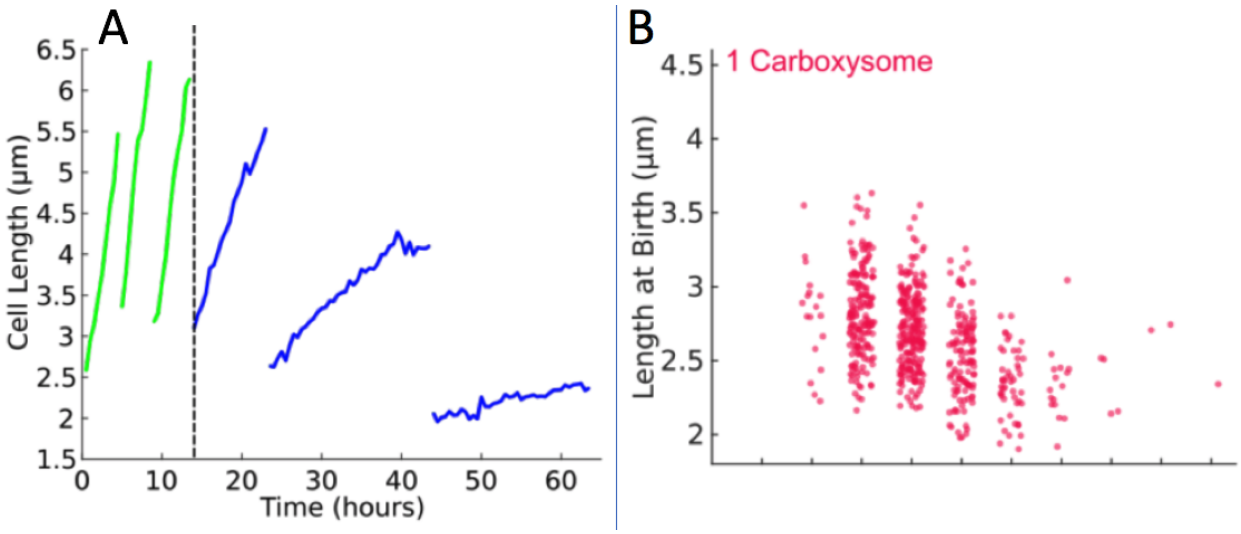

Figure 3.1: (A) Cell length over time for a cyanbacterial cell lineage. No new carboxysomes are formed, and after the three generations shown in bright green, the dark blue cells to the right of the vertical dashed line are all grown from the same single carboxysome. (B) Length at birth over generations, separated by bars, for cell lineages grown from one carboxysome. Images from [41].

each individual has the exact same likelihood of reproducing or dying, a structured model allows for finer precision in that individuals are characterized by discrete classes or continuous physiological properties—the structure variables. In the context of cell biology, individuals are traditionally characterized by age and/or size, which are generally good proxies for determining where a cell is in the cell cycle.

Carboxysome efficacy determines photosynthetic capability in cyanobacteria at both an individual and population level [41]. As these microstructures persist through multiple division cycles, carboxysome ages, a proxy for efficacy, are included as structure variables in the multi-structured model, along with cell size and chronological age. The main contribution of this work is in demonstrating that key model features, such as, the existence of a stable distribution in population structure, are maintained upon extending existing age and size structured models to include an arbitrary (but finite) number of additional structure variables. The model presented here is derived from three principal sources; these are, the age and size structured models presented by George I. Bell [10] and Henk Heijmans [47], as well as Susan Tucker and Stuart Zimmerman's nonlinear model [63].

The multi-structured model describes a population of cells structured by age $a \in \mathbb{R}_+ = [0, \infty)$, and k additional structure variables, x_i, stored in the vector $\bar{\mathbf{x}} \in \Omega \subset \mathbb{R}^k$. Let $x_1 \in (x_m, x_M]$ represent cell size, where x_m is the lower bound, and x_M is the maximum allowable size. In this application, x_1 will refer to length, but cell size is commonly measured as volume as well. The remaining $k-1$ structure variables, $\mathbf{x} = x_2, x_3, \cdots, x_k \in \mathbb{R}_+^{k-1}$, represent carboxysome ages, the number of which may vary depending on strain and environment. However, at the individual level, the number of carboxysomes per cell, $k-1$ is fixed. Vectors

in state space Ω are constructed in the following manner,

$$\bar{\mathbf{x}} = \begin{bmatrix} x_1 \\ \mathbf{x} \end{bmatrix} = \begin{bmatrix} x_1 \\ x_2 \\ x_3 \\ \vdots \\ x_k \end{bmatrix} = \begin{bmatrix} \text{Cell Length} \\ \text{Age of Carboxysome 1} \\ \text{Age of Carboxysome 2} \\ \vdots \\ \text{Age of Carboxysome } k-1 \end{bmatrix}.$$

Age is kept separate from the remaining physiological features to maintain clarity in the renewal condition at the age $a = 0$ boundary. It will also be necessary at times to refer to age and cell length separately from carboxysome ages, particularly when defining characteristic curves, hence the assigned notation [1] .

The population density, $n(t, a, \bar{\mathbf{x}})$, is naturally defined on $L^1(\mathbb{R}_+ \times \mathbb{R}_+ \times \Omega)$ as we assume a finite population size such that integrating over all ages and structure variables,

$$\int_0^\infty \int_\Omega n(t, a, \bar{\mathbf{x}}) d\bar{\mathbf{x}} da,$$

gives the total number of individuals at any time t.

3.1.2 Definition and interpretation of model components

Let $\mu(a, \bar{\mathbf{x}}) = d(a, \bar{\mathbf{x}}) + b(a, \bar{\mathbf{x}})$ be the *age- and state-specific rate of cell loss* due to death, $d(a, \bar{\mathbf{x}})$, and division, $b(a, \bar{\mathbf{x}})$. We assume that cell division is entirely symmetric in the structure variables, meaning, for each structure variable, both daughter cells inherit exactly one half of the mass or productivity its mother had at the time of division. The *birth modulus*, $\beta(a, \bar{\mathbf{y}}, \bar{\mathbf{x}})$, gives the average number of daughter cells of state $\bar{\mathbf{x}}$ produced per mother cell of age a and state $\bar{\mathbf{y}}$. In this model, mitosis is an instantaneous event resulting in the disappearance of the mother cell of state $\bar{\mathbf{y}}$, and two daughter cells of state $\bar{\mathbf{x}} = \frac{1}{2}\bar{\mathbf{y}}$ appearing at the $a = 0$ boundary.

[1] A note on notation: throughout this document, an overbar on a bolded variable, e.g., $\bar{\mathbf{x}}$, refers to a vector containing all k structure variables (length and carboxysome ages), whereas a bolded variable with no bar, e.g., $\mathbf{x}$, represents the $k-1$ carboxysome ages separately.

To be clear, this means that both of the two daughter cells inherit one half of the quantity their mother had of each structural variable. In previous applications, structure variables have stood for DNA or RNA mass. For our application, however, we measure carboxysome age as a proxy for photosynthetic capacity—the speed with which light is converted to biomass. Dividing this quantity between daughter cells allows us to maintain a fixed number of carboxysomes in the model, in that, for each carboxysome inherited at birth, a new full-capacity carboxysome is formed prior to division. With this assumption, daughter cells are born with approximately half the photosynthetic capability of their mothers. In Section 7.2 we propose some adaptations which may lead to a higher fidelity model of carboxysome aging and inheritance.

Furthermore, the symmetric division assumption imposes a partition of the state space into a region of cells large enough to divide, $\Omega_m = (\frac{x_M}{2}, x_M] \times \mathbb{R}_+^{k-1} \subset \Omega$, and a region Ω_b restricted to the allowable states at birth $\Omega_b = (x_m, \frac{x_M}{2}] \times \mathbb{R}_+^{k-1} \subset \Omega$. The birth modulus is then a Dirac-delta function applied to each structure variable of the form,

$$\beta(a, \bar{\mathbf{y}}, \bar{\mathbf{x}}) = 2\beta_1(a)\delta(\bar{\mathbf{x}} - \frac{1}{2}\bar{\mathbf{y}}) \text{ for } \bar{\mathbf{x}} \in \Omega_b,\ \bar{\mathbf{y}} \in \Omega_m, \tag{3.1}$$

and $\beta_1(a)$ a condition for age-at-division. Integrating the birth modulus over Ω_b with respect to $\bar{\mathbf{x}}$ gives the total average number of daughter cells produced per unit time by a mother cell of age a and state $\bar{\mathbf{y}}$. Therefore, the rate of cell loss due to division is,

$$\begin{aligned} b(a, \bar{\mathbf{y}}) &= \frac{1}{2}\int_{\Omega_b} \beta(a, \bar{\mathbf{y}}, \bar{\mathbf{x}}) d\bar{\mathbf{x}} \\ &= \frac{1}{2}\int_{\Omega_b} 2\beta_1(a)\delta(\bar{\mathbf{x}} - \frac{1}{2}\bar{\mathbf{y}}) d\bar{\mathbf{x}} \\ &= \beta_1(a)\chi_{\{\bar{\mathbf{y}} \in \Omega_m\}}, \end{aligned} \tag{3.2}$$

where $\chi_{\{\bar{\mathbf{y}} \in \Omega_m\}}$ is the indicator function on Ω_m. The factor of $\frac{1}{2}$ balances the removal of a dividing mother cell with her two daughter cells—as in, the rate at which offspring are produced is twice the rate of cell loss due to division. Assuming a constant death rate,

$d(a, \bar{\mathbf{y}}) = \mu_d$, the total loss rate becomes,

$$\mu(a, \bar{\mathbf{y}}) = \mu_d + \beta_1(a)\chi_{\{\bar{\mathbf{y}} \in \Omega_m\}}. \tag{3.3}$$

Each structure variable x_i grows or evolves with velocity $v_i(a, \bar{\mathbf{x}}) = \dfrac{dx_i}{dt}(a, \bar{\mathbf{x}})$, forming the velocity vector $\bar{\mathbf{v}}(a, \bar{\mathbf{x}}) = [v_1(a, \bar{\mathbf{x}}) \;\; v_2(a, \bar{\mathbf{x}}) \;\; \cdots \;\; v_k(a, \bar{\mathbf{x}})]^T$. Velocity functions $v_i(a, \bar{\mathbf{x}})$ are required to be bounded, continuous, and continuously differentiable with respect to each of its arguments. Additionally, $v_i(a, \bar{\mathbf{x}})$ must be strictly positive on the interior of Ω, $\inf_{\{(a,\bar{\mathbf{x}}) \in (0,\infty)\times(x_m, x_M)\times(0,\infty)^k\}} |v_i(a, \bar{\mathbf{x}})| > 0$, to guarantee a uniquely determined flow along characteristic curves across Ω, and, $v_i(a, \bar{\mathbf{x}})$ must vanish on the boundary of Ω, $\partial\Omega$, so that all trajectories beginning at time t with $(a, \bar{\mathbf{x}}) \in \mathbb{R}_+ \times \Omega$, remain in $\mathbb{R}_+ \times \mathbb{R}_+ \times \Omega$.

3.1.3 Model equations

Accordingly, multi-structured population evolution follows the $(k+2)$-dimensional hyperbolic, linear PDE,

$$\begin{aligned} &\frac{\partial n}{\partial t} + \frac{\partial n}{\partial a} + \nabla \cdot [\bar{\mathbf{v}}(a, \bar{\mathbf{x}}) n(t, a, \bar{\mathbf{x}})] = -\mu(a, \bar{\mathbf{x}}) n(t, a, \bar{\mathbf{x}}) \\ &\quad n(t, 0, \bar{\mathbf{x}}) = B(t, \bar{\mathbf{x}}) = \int_0^\infty \int_{\Omega_d} \beta(a, \bar{\mathbf{y}}, \bar{\mathbf{x}}) n(t, a, \bar{\mathbf{y}}) d\bar{\mathbf{y}} da \\ &\quad n(0, a, \bar{\mathbf{x}}) = \phi(a, \bar{\mathbf{x}}) \end{aligned} \tag{3.4}$$

where

$$\nabla \cdot [\bar{\mathbf{v}}(a, \bar{\mathbf{x}}) n(t, a, \bar{\mathbf{x}})] = \sum_{i=1}^{k} \frac{\partial [\bar{\mathbf{v}}_i(a, \bar{\mathbf{x}}) n(t, a, \bar{\mathbf{x}})]}{\partial x_i}$$

is the divergence of the vector field $\bar{\mathbf{v}}(a, \bar{\mathbf{x}}) n(t, a, \bar{\mathbf{x}})$.

Since each velocity term $v_i(a, \bar{\mathbf{x}})$ is required to be continuously differentiable with respect to x_i, the balance law may be written as a directional derivative in the $\langle 1, 1, \bar{\mathbf{v}} \rangle$ direction,

$$D_{\langle 1,1,\bar{\mathbf{v}} \rangle} n(t, a, \bar{\mathbf{x}}) = -\left(\mu(a, \bar{\mathbf{x}}) + \sum_{i=1}^{k} \frac{\partial v_i}{\partial x_i}(a, \bar{\mathbf{x}}) \right) n(t, a, \bar{\mathbf{x}}), \tag{3.5}$$

giving the instantaneous rate of change at time t in the direction of aging and growth from every age and state in Ω. Ignoring the loss term $\mu(a, \bar{\mathbf{x}})$ for a moment, viewing the PDE this

form shows that the movement of population density from convection or transport (left of the equals sign), is balanced with the dilation or contraction of volume elements as individuals are translated through state space.

3.2 Solution via Method of Characteristics

3.2.1 Characteristic curves

Setting the right-hand-side of (3.5) equal to zero says that the rate of change in density n at any point $(t, a, \bar{\mathbf{x}})$ is zero in the $\langle 1, 1, \bar{\mathbf{v}} \rangle$ direction. A parameterized curve advancing from an initial position in the $\langle 1, 1, \bar{\mathbf{v}} \rangle$ direction, along which n is constant, is called a characteristic curve. Integrating along these curves produces a solution to the model (3.4) where the density at time t is expressed in terms of the initial data $\phi(a, \bar{\mathbf{x}})$ propagated forward in time along characteristics. The characteristic curves[2] for this system are solutions $T = T(\theta, t), A = A(\theta, a), X_1 = X_1(\theta, x_1)$, and $\mathbf{X} = \mathbf{X}(\theta, \mathbf{x})$ to the following system of differential equations parameterized by auxiliary variable θ, standing for time when $t \leq a$, and age when $t > a$.

$$\begin{aligned}
&\frac{d}{d\theta}[T(\theta, t)] = 1, \quad T(0, t) = t \\
&\frac{d}{d\theta}[A(\theta, a)] = 1, \quad A(0, a) = a \\
&\frac{d}{d\theta}[X_1(\theta, x_1; a, \mathbf{x})] = v_1(A(\theta, a), x_1, \mathbf{X}(\theta, \mathbf{x})), \quad X_1(0, x_1) = x_1 \\
&\frac{d}{d\theta}[X_i(\theta, x_i; a, x_{j \neq i})] = v_i(A(\theta, a), X_1(\theta, x_1), \mathbf{X}(\theta, \mathbf{x})), \quad X_i(0, x_i) = x_i
\end{aligned} \tag{3.6}$$

The characteristics along which time passes and age advances are given by,

$$T(\theta, t) = \theta + t \text{ and } A(\theta, a) = \theta + a.$$

For the characteristic curves describing cell growth,

$$\frac{d}{d\theta}[X_1(\theta, x_1; a, \mathbf{x})] = v_1(A, x_1, \mathbf{X}) \;\Rightarrow\; \int_{x_1}^{X_1} \frac{d\xi}{v_1(A, \xi, \mathbf{X})} = \theta$$

[2] Capital letters are used to refer to characteristic curves. Generally, these will be presented with two arguments, as in $X(\theta, x)$, however, the characteristics in state space may also depend on age and other structure variables, considered to be fixed, and will be denoted explicitly by $X(\theta, x; a, \mathbf{x})$ only when necessary.

Let $G(x) = G(x; a, \mathbf{x}) = \int_{x_m}^{x} \frac{d\xi}{v_1(A(\theta, a), \xi, \mathbf{X}(\theta, \mathbf{x}))}$, the *time* required for a cell of age a and state $\mathbf{x}$ to grow from the smallest possible size x_m to arbitrary size $x \leq x_M$. A cell of *fixed* size x_1 at time t, will reach arbitrary size $x \leq x_M$ a time $G(x) - G(x_1)$ later. Continuing from the above,

$$\theta = \int_{x_1}^{X_1} \frac{d\xi}{v_1(A, \xi, \mathbf{X})} = \int_{x_m}^{X_1} \frac{d\xi}{v_1(A, \xi, \mathbf{X})} - \int_{x_m}^{x_1} \frac{d\xi}{v_1(A, \xi, \mathbf{X})}$$

$$\theta = G(X_1) - G(x_1) \;\Rightarrow\; G(X_1) = \theta + G(x_1)$$

$$X_1(\theta, x_1) = G^{-1}(\theta + G(x_1)).$$

The inverse, $G^{-1}(\theta; x_1) = G^{-1}(\theta; a, x_1, \mathbf{x})$, is guaranteed to exist as long as the physical growth rate $v_1 : [x_m, x_M] \to \mathbb{R}_+$ is uniformly continuous and positive on $[x_m, x_M]$. $G^{-1}(\theta; x_1)$ is called the *growth curve* as it computes the *size* of an individual after a time period of length θ. For instance, an individual of size x_1 at time t_0 will be of size $G^{-1}(\theta; x_1)$ at time $t_0 + \theta$. It is helpful to note that $G^{-1}(0; x_1) = x_1$.

For each additional structure variable in $\mathbf{x}$, the characteristic curves $X_i(\theta, x_i; a, x_{j\neq i})$ will be similarly expressed through integral equations. While by definition $v_i(a, x_1, \mathbf{x})$ should be 1 if x_i represents carboxysome age, velocity functions are not required to be positive, and it's worthwhile to lay the framework for replacing $v_i(a, x_1, \mathbf{x})$ with a more direct measure of carboxysome efficacy in the future.

$$\frac{d}{d\theta}[X_i(\theta, x_i; a, x_{j\neq i})] = v_i(A(\theta, a), X_1(\theta, x_1), \mathbf{X}(\theta, \mathbf{x})) \;\Rightarrow\; \int_{x_i}^{X_i} \frac{d\xi}{v_i(A, X_1, \bar{\mathbf{X}}|_{x_i=\xi})} = \theta$$

Let $F_i(x) = F_i(x; a, \mathbf{x}) = \int_{0}^{x} \frac{d\xi}{v_i(A, X_1, \mathbf{x}|_{x_i=\xi})}$, be the *time* required for the i^{th} carboxysome initially of age zero to reach age x along the characteristic curve.

$$\theta = \int_{0}^{X_i} \frac{d\xi}{v_i(A, X_1, \bar{\mathbf{X}}|_{x_i=\xi})} = \int_{0}^{X_1} \frac{d\xi}{v_i(A, X_1, \bar{\mathbf{X}}|_{x_i=\xi})} - \int_{0}^{x_1} \frac{d\xi}{v_i(A, X_1, \bar{\mathbf{X}}|_{x_i=\xi})}$$

$$\theta = F_i(X_i) - F_i(x_i) \;\Rightarrow\; F_i(X_i) = \theta + F_i(x_i)$$

$$X_i(\theta, x_i) = F_i^{-1}(\theta + F_i(x_i)).$$

The inverse functions, $F_i^{-1}(\theta; x_i) = F_i^{-1}(\theta; a, x_1, \mathbf{x})$, are again guaranteed to exist as long as $v_i : \mathbb{R}_+ \to \mathbb{R}_+$ is positive and uniformly continuous on $\mathbb{R}_+$. $F_i^{-1}(\theta; x_i)$ should be interpreted as the age of a carboxysome after a time period of length θ.

Consider a cell of age a and state $\bar{\mathbf{x}}$. The vector $\bar{\mathbf{X}}(\theta, \bar{\mathbf{x}})$ is the vector of characteristic curves advancing the cell to its next state $\bar{\mathbf{X}}$, after a time interval of length θ. A cell's state-at-birth $\bar{\mathbf{X}}(-a, \bar{\mathbf{x}})$ can always be found by traveling backwards along a characteristic curve for a time a.

3.2.2 Exponential growth model for cell length

Exponential growth is a biologically reasonable assumption for the majority of cell populations, including cyanobacteria [18]. Under this assumption, cell size increases in proportion to itself at a rate $\alpha(\mathbf{x})$. The growth rate could be constant, in which case $\alpha(\mathbf{x}) = \alpha$, or have an inverse relationship with carboxysome age wherein the maximum growth rate $\alpha = \alpha(\mathbf{x} = \mathbf{0})$, and $\lim_{a\to\infty} \alpha(\mathbf{x}) = 0$.

In this model, cell growth is according to $\dfrac{dx_1}{dt} = v_1(A, x_1, \mathbf{X}(a, \mathbf{x})) = \alpha(\mathbf{X}(a, \mathbf{x}))x_1$. Consider a cell that was of size x_m at age $a = 0$ with carboxysome ages $\mathbf{x}$. The time required for that cell to grow to size x is,

$$G(x) = \int_{x_m}^{x} \frac{d\xi}{v_1(A, \xi, \mathbf{X}(a, \mathbf{x}))} = \int_{x_m}^{x} \frac{d\xi}{\alpha(\mathbf{X}(a, \mathbf{x}))\xi} = \frac{1}{\alpha(\mathbf{X}(a, \mathbf{x}))} \ln(x/x_m).$$

The size of that cell after a time period of length t is, $G^{-1}(t; x_1) = x_m e^{t\alpha(\mathbf{X}(a=0,\mathbf{x}))}$, and the characteristic curve for cell length is then $X_1(t, x_1; \mathbf{x}) = x_1 \exp[t\alpha(\mathbf{X}(a, \mathbf{x}))]$. Carboxysomes age with velocity $v_i = 1$, along characteristic curves $X_i(a, x_i) = x_i + a$.

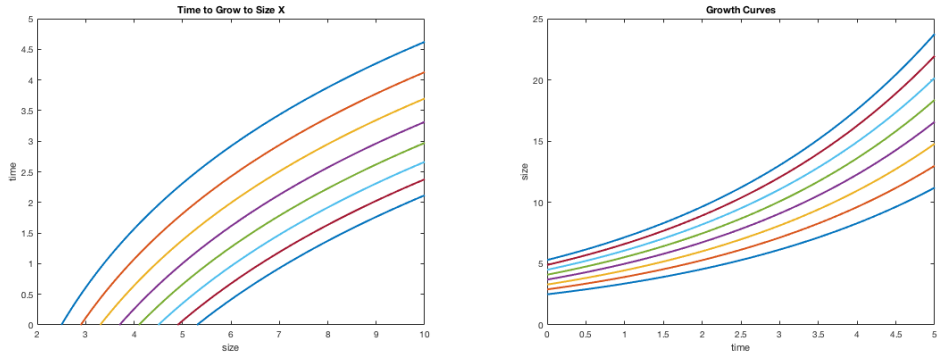

Figure 3.2: **Left**: $G_1(X_1) - G_1(x_0)$, the *time* required for cells to grow from initial sizes x_0 to an arbitrary size X_1. **Right**: The growth curves, $G_1^{-1}(t)$, or size at time t, for various values of initial cell size x_0.

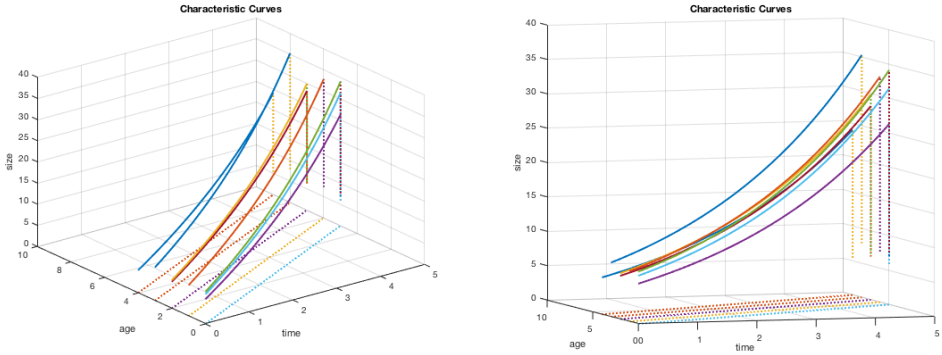

Figure 3.3: Two views of the characteristic curves $X_1(\theta, x_1)$. Notice that projections of $X_1(\theta, x_1)$ onto the at-plane are lines of slope 1, consistent with $\frac{da}{dt} = 1$.

3.3 Model Solutions

We obtain a solution for $n(t, a, \bar{\mathbf{x}})$ by integrating the total derivative of n along characteristic curves, as in,

$$\frac{d}{d\theta}\left[n(T(\theta,t), A(\theta,a), \bar{\mathbf{X}}(\theta,\bar{\mathbf{x}}))\right] = \frac{\partial n}{\partial t}\frac{dt}{d\theta} + \frac{\partial n}{\partial a}\frac{da}{d\theta} + \sum_{i=1}^{k}\frac{\partial n}{\partial x_i}\frac{dx_i}{d\theta}$$

which we recognize from the model equations (3.4) to be equivalent to,

$$\frac{dn}{d\theta} = -\left(\mu(A,\bar{\mathbf{X}}) + \sum_{i=1}^{k}\frac{\partial v_i}{\partial x_i}(A,\bar{\mathbf{X}})\right)n(T,A,\bar{\mathbf{X}}),$$

with solution,

$$n(T,A,\bar{\mathbf{X}}) = C\exp\left[-\int_0^\theta \mu(A,\bar{\mathbf{X}})d\theta' - \int_0^\theta\sum_{i=1}^{k}\frac{\partial v_i}{\partial x_i}(A,\bar{\mathbf{X}})d\theta'\right].$$

To find the constant term C, we divide the at-plane along the line $a = t$. In the region where $t < a$, our solution propagates the initial distribution $n(0, a, \bar{\mathbf{x}}) = \phi(a, \bar{\mathbf{x}})$ forward in time, and in the region where $t \geq a$, the boundary condition $n(t, 0, \bar{\mathbf{x}})$ dispenses a distribution at the age $a = 0$ boundary that is then propagated forward as well. Let

$$\Pi(s; a, \bar{\mathbf{x}}) = \exp\left[-\int_0^s \mu(a - s + \sigma, \bar{\mathbf{X}}(\sigma - s, \bar{\mathbf{x}}))d\sigma\right]$$

be the *survival probability*, the probability that a cell of age a and state $\bar{\mathbf{x}}$ at time t will remain in the population at time $t + s$, that is, the cell will not have died or divided during the time interval of length s. For an age-structured model, the survival probability is sufficient to determine the density of a cell cohort over time. However, for the multi-structured model, we must also resolve how the volume occupied by a given cohort is distorted as it is translated through state space. The volume distortion is illustrated in Figure 3.4 below. The Jacobian,

$$J(s; a, \bar{\mathbf{x}}) = \exp\left[-\int_0^s\sum_{i=1}^{k}\frac{\partial v_i}{\partial X_i}d\sigma\right] = \left|\frac{\partial(A(s,a), \bar{\mathbf{X}}(s,\bar{\mathbf{x}}))}{\partial(a,\bar{\mathbf{x}})}\right|,$$

is the determinant of the Jacobian matrix for the characteristic curves (see Appendix A for proof). The Jacobian term may be interpreted as a coordinate transformation in time, that

is, from the current time to a small time s later on [3]. Said another way, this term accounts for the fact that a cohort occupying a volume V initially will grow to occupy a volume that is larger by a factor of $\exp\left[\int_0^s \sum_{i=1}^{k} \frac{\partial v_i}{\partial X_i} d\sigma\right]$ at time s [10].

Finally, we arrive at the following solution for the population density,

$$n(t,a,\bar{\mathbf{x}}) = \begin{cases} \phi(a-t, \bar{\mathbf{X}}(-t,\bar{\mathbf{x}}))\Pi(t)J(t) & \text{for } t < a \\ n(t-a,0,\bar{\mathbf{X}}(-a,\bar{\mathbf{x}}))\Pi(a)J(a) & \text{for } t > a. \end{cases} \tag{3.7}$$

In the region where $t < a$, the solution is fully determined from the initial condition. As an example, Figure 3.5 shows the evolution of the age and size distribution of a cohort of cells beginning at time $t = 0$. Resolving the boundary condition, however, may not be possible in a closed form.

3.4 Series solution

To obtain the solution to (3.4) where $0 \leq a < t$, the piecewise-defined solution for n is inserted into the boundary condition,

$$n(t,0,\bar{\mathbf{x}}) = B(t,\bar{\mathbf{x}}) = \int_0^\infty \int_\Omega \beta(a,\bar{\mathbf{y}},\bar{\mathbf{x}}) n(t,a,\bar{\mathbf{y}}) d\bar{\mathbf{y}} da,$$

resulting in the following integral equation for the birth-rate function $B(t,\bar{\mathbf{x}})$.

$$\begin{aligned} B(t,\bar{\mathbf{x}}) &= \int_0^t \int_\Omega \beta(a,\bar{\mathbf{y}},\bar{\mathbf{x}}) B(t-a, \bar{\mathbf{Y}}(-a,\bar{\mathbf{y}})) \exp\left[-\int_0^a \mu(\sigma, \bar{\mathbf{Y}}(\sigma-a,\bar{\mathbf{y}}))d\sigma\right] J(a) d\bar{\mathbf{y}} da \\ &+ \int_t^\infty \int_\Omega \beta(a,\bar{\mathbf{y}},\bar{\mathbf{x}}) \phi(a-t, \bar{\mathbf{Y}}(-t,\bar{\mathbf{y}})) \exp\left[-\int_0^t \mu(a+\sigma-t, \bar{\mathbf{Y}}(\sigma-t,\bar{\mathbf{y}}))d\sigma\right] J(t) d\bar{\mathbf{y}} da \\ &= K(B)(t,\bar{\mathbf{x}}) + \Phi(t,\bar{\mathbf{x}}) \end{aligned} \tag{3.8}$$

The above equation may be simplified slightly by a change of variables. The Jacobian term acts as a coordinate transformation on Ω from a time dt ago to the present. The Jacobian matrix used to change of variables from the past, $\bar{\mathbf{Y}}(-t,\bar{\mathbf{y}})$ to current-time coordinates,

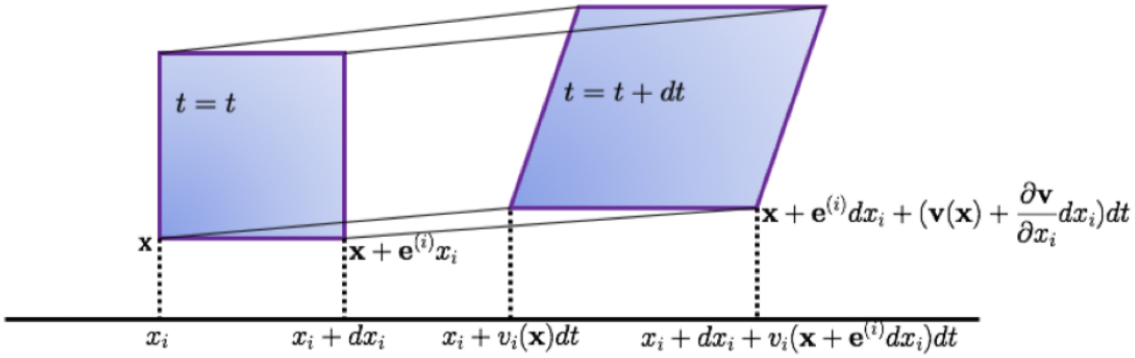

Figure 3.4: This figure depicts the deformation in state space as a cohort of cells increases in volume as it moves through the space. A cohort of cells originally occupying an area of x^2 will grow to occupy and area of $x^2 e^{\alpha t}$ as it ages from age a to $a + t$. The Jacobian accounts for this expansion to maintain a constant density along characteristic curves. In other words, propagating a cohort forward in time can be thought of as a coordinate transformation in state space from $\bar{\mathbf{x}} \to \bar{\mathbf{X}}(t, \bar{\mathbf{x}})$.

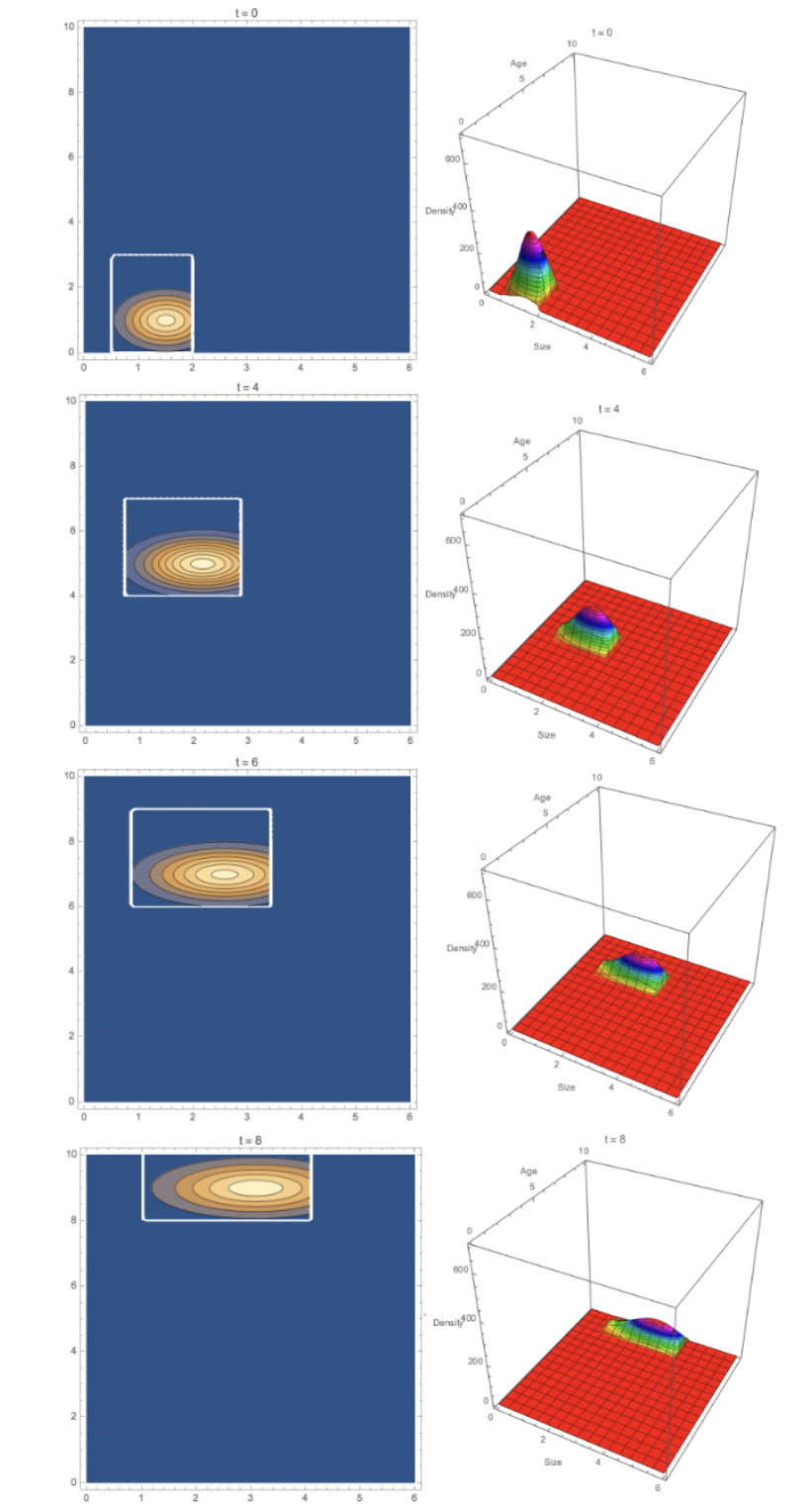

Figure 3.5: A forward simulation of the semigroup solution applied to the age and size distribution of an initial cohort of cells drawn from a multivariate-normal distribution.

$\bar{\mathbf{Y}}(t, \bar{\mathbf{y}})$, is exactly the inverse of the Jacobian in the solution. The integral equation for $B(t, \bar{\mathbf{x}})$ is equivalently expressed,

$$\begin{aligned} B(t, \bar{\mathbf{x}}) &= \int_0^t \int_\Omega \beta(a, \bar{\mathbf{Y}}(a, \bar{\mathbf{y}}), \bar{\mathbf{x}}) B(t-a, \bar{\mathbf{y}}) \exp\left[-\int_0^a \mu(\sigma, \bar{\mathbf{Y}}(\sigma, \bar{\mathbf{y}})) d\sigma \right] d\bar{\mathbf{y}} da \\ &+ \int_0^\infty \int_\Omega \beta(a+t, \bar{\mathbf{Y}}(t, \bar{\mathbf{y}}), \bar{\mathbf{x}}) \phi(a, \bar{\mathbf{y}}) \exp\left[-\int_0^t \mu(a+\sigma, \bar{\mathbf{Y}}(\sigma, \bar{\mathbf{y}})) d\sigma \right] d\bar{\mathbf{y}} da \qquad (3.9) \\ &= K(B)(t, \bar{\mathbf{x}}) + \Phi(t, \bar{\mathbf{x}}). \end{aligned}$$

The first integral behaves as an operator acting on B, call this operator K and the integral $K(B)(t, \bar{\mathbf{x}})$. The second integral depends on the initial condition and will be labeled $\Phi(t, \bar{\mathbf{x}})$.

The proof of the following existence and uniqueness theorem shows that the integral equation (3.8) for B has a solution $B(t, \cdot)$ which admits a continuous mapping for t in the interval $[0, T]$ to the state space Ω, and that this mapping can be extended to the full space as $t \to \infty$. Though we may not find a closed form solution for B, the method of successive approximations gives a solution in the form of a convergent series of repeated applications of the operator K to the initial cohort Φ. In this way, each application of K corresponds to the next generation of cells.

Theorem 1. *There exists a unique, continuous and bounded solution B to (3.9).*

Proof. Let $\Omega_1 \subset \Omega$ be the volume of state space occupied by the initial cohort, and $\tilde{\beta}$ an upper bound on the birth modulus. (Refer to the integral equations as presented in (3.8) to see clearly how the Jacobian increases Ω_1 with each application of K.) The operator K is continuous in t and $\bar{\mathbf{x}}$, and bounded in sup norm by,

$$||K|| \leq t\tilde{\beta}\Omega_1 \sup_{0 \leq \sigma \leq t} ||B||.$$

Φ is also continuous in t and $\bar{\mathbf{x}}$, and bounded by, $||\Phi|| \leq \tilde{\beta}||\phi||_{L^1}$. By the method of successive approximations,

$$B = \Phi + K(\Phi) + K^2(\Phi) + \cdots = \sum_{N=0}^{\infty} K^N(\Phi).$$

The series solution for B converges on an interval $[0, T \leq \frac{1}{\tilde{\beta}\Omega_1}]$ as repeated applications of K, each representing the next newly born cohort of cells, remain bounded

$$||K^N(\Phi)|| \leq (T\tilde{\beta}\Omega_1)^N \cdot \tilde{\beta}||\phi||_{L^1}.$$

Since B is the uniform limit of continuous functions, it is also continuous. Assuming there are two solutions, B_1 and B_2, and inserting their difference $B_1 - B_2$ into the above inequality in place of Φ shows that this solution is unique as well. □

We have shown that a unique and continuous solution B to the integral equation

$$B(t, \bar{\mathbf{x}}) = K(B)(t, \bar{\mathbf{x}}) + \Phi(t, \bar{\mathbf{x}}), \tag{3.10}$$

exists, and can by approximated by a power series. The series converges to the solution B on a closed time interval, however, the length of the interval grows with the addition of each new term, or generation. In other words, we can always find the distribution of newborn cells as the sum of the contribution, determined through K, from all of the previous cohorts, and the population will become infinitely large in infinite time—which is eventually how long it would take to add all of this up. Nevertheless, we will still be able to extract valuable information about the long-term behaviour of the population, particularly, if a stable distribution is reached in age and within the structure variables, even while the population continues to grow in time.

3.5 Asymptotic Behavior

We conclude this chapter with a brief discussion of what it means to find an asymptotic (long-term) solution. An asymptotic solution describes the behavior of a system as time increases to infinity. Generally, there is a short, transient phase before the promised asymptotic behavior is realized, the challenge is in separating out the dominant behavior that will persist over time and showing that all other contributions quickly become negligible. The asymptotic solution is analogous to an equilibrium solution for a linear model in

that, the population will continue to increase for all time (or go extinct) while the fraction of the total population of a given state remains constant.

If such a solution exists, evolution in time can be separated from the structural distribution yielding solutions $B(t, \bar{\mathbf{x}})$ of the form

$$B(t, \bar{\mathbf{x}}) = e^{\lambda t}\psi(a, \bar{\mathbf{x}}),$$

where the constant λ is the Malthusian growth parameter, intrinsic to the population itself. Due to the formulation of our model, there are two approaches one could use to arrive at this type of result, and we will show that under certain conditions on cell growth, the multi-structured model admits a (periodic) steady-state solution.

In the first approach, we will show that the PDE (3.4) is the generator of a strongly continuous semigroup. The boundary condition is interpreted as a perturbation to the generator of this semigroup by a bounded linear operator, and analysis of the spectral properties of this operator determine conditions for a steady-state solution. In the second approach, we view (3.10) as an abstract renewal equation and solve the eigenproblem for the eigenvalue λ and eigenfunction ψ, which again determine conditions for a steady-state solution for B. Finally, we discuss how the two approaches are linked, what it means to arrive at a periodic steady-state solution, and what is gained from this analysis.

Chapter 4

Semigroup Approach

From the semigroup point of view, the evolution of a structured population is cast as a dynamical system in state-space. That is to say, rather than our previous understanding of the model PDE (3.4) through a directional derivative, as in Equation (3.5), we move everything except the rate of change in density with respect to time, $\frac{\partial}{\partial t}n(t, a, \bar{\mathbf{x}})$, to the right-hand-side, and consider this, the sum of all of the changes to the density occurring in state-space, as a *linear operator* acting on the state-space. This leads to an abstract formulation of the dynamical system in state-space, which has a family strongly-continuous linear operators, called a semigroup, as its solution. A semigroup is analogous to a matrix exponential, and we will see that it has many of the same nice continuity properties and functions in much the same way. However, one of the major advantages a semigroup solution offers is that, unlike a classical PDE solution, a semigroup solution may be perturbed to include discontinuous jumps in state-space. In constructing a solution for our model, cell division will be included as one such jump discontinuity in that a dividing cell is removed from the population only to instantaneously reappear as a transformation of itself at the age $a = 0$ boundary.

In this chapter, we present some of the key theorems and concepts from semigroup theory, and apply them to find the semigroup solution of our model. We then show that the boundary condition may be resolved by a perturbation to the semigroup solution, and conclude by deriving the eigenproblem (to be solved in Chapter 6) whose solutions determine

the asymptotic behavior of the population.

4.1 Semigroup Solution and Properties

We show that the solution obtained by the method of characteristics is a strongly-continuous semigroup of linear operators acting on the state space. Analysis of the semigroup and its generator describe the long-term, or asymptotic, behavior of the population. For this linear model, the population will either reach the locally asymptotically stable zero solution, or grow infinitely large in infinite time. Neither of these options are particularly captivating, unless we can show that the population exhibits some structural organization along the way. The aim of this section is to characterize this behavior through asymptotic analysis. In this section, a brief overview of the theory and its utility will be presented. We define well-posedness of the Abstract Cauchy Problem (ACP) and establish spectral properties of generators of strongly continuous semigroups. We then turn our attention to the multi-structured model (3.4) and establish that this theory applies to the problem under consideration by explicitly stating and proving well-posedness of the ACP and semigroup solution.

In the semigroup formulation, we think of a PDE, such as (3.4), as being associated with a linear operator $\mathcal{A}$ acting on a Banach space U. That is, the state of our population density at any time t is identified with a point in the Banach space $U = L^1(\mathbb{R}_+ \times \Omega)$, and the semigroup, said to be *generated* by $\mathcal{A}$, is the continuous map from any initial state $\phi_1(a, \bar{\mathbf{x}}) \in U$ to the state $\phi_2(a, \bar{\mathbf{x}}) \in U$ at time t. As an illustrative example, consider the Malthusian growth model for a population $n(t)$. The population evolves according to the ODE

$$\frac{dn(t)}{dt} = \lambda n, \quad n(0) = \phi.$$

The operator $\mathcal{A}$ in this case is simply the constant λ, and the semigroup it generates is $e^{\lambda t}$. The solution to this ODE is $n(t) = \phi e^{\lambda t}$, from which it is clear to see that the semigroup,

$e^{\lambda t}$, maps an initial state ϕ to the state at any future time t. But, it is the properties of $\mathcal{A}$ that dictate the fate of this population in that, if $\lambda > 0$, the population grows to infinity in infinite time, and if $\lambda < 0$, the population will die out.

4.2 The Abstract Cauchy Problem

In an entirely analogous way, the time evolution of $n(t, a, \bar{\mathbf{x}})$ is described by a function mapping $t \in \mathbb{R}_+ \to n(t, \cdot, \cdot) \in U$, governed by the ACP,

$$\frac{dn(t)}{dt} = \mathcal{A}n(t), \quad n(0) = \phi \tag{ACP}$$

where $\mathcal{A}$ is a linear, closed, and generally unbounded (differential) operator with dense domain $\mathcal{D}(\mathcal{A}) \in U$ [52]. The word *abstract* in Abstract Cauchy Problem signifies that solutions are Banach space valued.

A function $n : \mathbb{R}_+ \to U$ is a solution of (ACP) if it is continuously differentiable, takes on values in $\mathcal{D}(\mathcal{A})$, and satisfies the ACP. The ACP is *well-posed* if for every initial state $\phi \in \mathcal{D}(\mathcal{A})$, there exists a unique solution with continuous dependence on ϕ. Solutions of a well-posed ACP give rise to a family $\{S(t)\}$ of bounded linear operators on U, defined as the unique set of operators satisfying $n(t) = S(t)\phi$ [38]. Finally, this family of operators $\{S(t)\}$ is a *strongly-continuous semigroup*, meaning, it satisfies the following four defining properties (reminiscent of how exponentials behave):

(1) $S(t)$ is a continuous mapping from U into itself.

(2) $S(0) = I$.

(3) The semigroup property, $S(s)S(t)\phi = S(t + s)\phi$.

(4) Strong continuity, $\lim_{t \searrow 0} ||S(t)\phi - \phi|| = 0$.

On the other hand, each semigroup can be associated with a closed, densely defined

operator $\mathcal{A}$ called the *infinitesimal generator*, or simply the *generator*, of S, defined

$$\mathcal{A}\phi = \lim_{t \searrow 0} \frac{1}{t}(S(t)\phi - \phi). \tag{4.1}$$

The operator $\mathcal{A}$ uniquely determines the semigroup, and gives rise to a well-posed ACP [52]. The relationship between the ACP, a semigroup, and its generator is summarized by the Well-Posedness Theorem [51], [38]:

Theorem 2. *Well-Posedness Theorem. For a closed linear operator $\mathcal{A}$ with domain $\mathcal{D}(\mathcal{A})$ dense in a Banach space U, the following properties are equivalent:*

(1) The ACP defined on B is well-posed.

(2) The operator $\mathcal{A}$ is the generator of a strongly-continuous semigroup $\{S(t)\}_{t\geq 0}$ on B, and classical solutions of the ACP are given by $n(t) = S(t)\phi$ for $\phi \in \mathcal{D}(\mathcal{A})$.

4.3 Spectral Properties of the Generator

While the ultimate goal is to solve (ACP), it is the spectral properties of the generator $\mathcal{A}$ that give us an idea of the asymptotic behavior of solutions. This is made clear by the Hille-Yosida Theorem, the central theorem of semigroup theory which distiguishes the generators of strongly continuous semigroups among the class of all linear operators. This theorem has many formulations, stated here is the version appearing in [64]. And, as in [64], we first make the observation that every strongly continuous semigroup is *exponentially bounded* which follows from semigroup property (III) above.

Lemma 3. *Let $\mathcal{A}$ be a linear operator on a Banach space U, let $S(t)$ be a strongly continuous semigroup, and let $\omega \in \mathbb{R}$, and $M \geq 1$ be constants. Then the following two properties hold.*

(1) $S(t)$ is generated by $\mathcal{A}$ and satisfies $||S(t)|| \leq Me^{\omega t}$ for all $t \geq 0$.

Proof. Choose $M \geq 1$ such that $||S(s)|| \leq M$ for all $0 \leq s \leq 1$ and write $t \geq 0$ as $t = s + n$ for $n \in \mathbb{N}$ and $0 \leq s < 1$. Then,

$$\begin{aligned} ||S(t)|| &\leq ||S(s)|| \cdot ||S(1)||^n \leq M^{n+1} \\ &= Me^{n\ln(M)} \leq Me^{\omega t} \end{aligned}$$

holds for $\omega := \ln(M)$ and each $t \geq 0$ [32]. □

(2) $\mathcal{A}$ is closed, and densely defined on U. The half-line (ω, ∞) is contained in the resolvent set $\rho(\mathcal{A})$, and we have the estimates,

$$||R(\lambda, \mathcal{A})^m|| \leq \frac{M}{(Re(\lambda) - \omega)^m}, \quad \forall \lambda > \omega, \quad m \in \mathbb{N}.$$

Proof. By the Hille-Yosida Theorem [52]. □

The fact that the second property implies the first means that spectral properties of $\mathcal{A}$ signify the existence of a corresponding semigroup S, and well-posedness of the associated ACP. The question is, which spectral properties of $\mathcal{A}$ will allow us to make conclusions about the asymptotic behavior of S, and thus the solutions of the ACP. Of particular interest are the *spectrum of an operator*, the *resolvent set*, the *resolvent operator*, and the *spectral radius* defined in Appendix C.

The primary result from the spectral properties of the generator, $\mathcal{A}$, is that it allows us to establish a growth bound on the semigroup it generates, and therefore on solutions to the associated ACP. The uniform growth bound, $\omega_0(S)$, is defined as

$$\omega_0(S) := \inf\{\omega \in \mathbb{R} : \exists M > 0 \text{ such that } ||S(t)|| \leq Me^{\omega t}, \forall t \geq 0\}.$$

From the Hille-Yosida Theorem, we have that the spectrum of the generator of a strongly continuous semigroup is always contained in some left half-plane, as in, the maximum real part of an element of the spectrum defines an infinite vertical boundary (an abscissa) and

all other elements in the spectrum of the generator are contained in the half-plane to the left of this boundary. We can then define the spectral bound $s(\mathcal{A})$ by

$$s(\mathcal{A}) := \sup\{Re(\lambda) : \lambda \in \sigma(\mathcal{A})\}.$$

Furthermore, the Perron-Frobenius Theorem for positive semigroups states that, for a positive semigroup, $s(\mathcal{A})$ is always in the spectrum of $\mathcal{A}$ [38].

The Spectral Mapping Theorem states that, for a linear operator L, and an analytic function f,

$$\sigma(f(L)) = f(\sigma(L)).$$

The Taylor series for an exponential function is everywhere convergent, so that $\sigma(e^{t\mathcal{A}})$ is equal to $e^{t\sigma(\mathcal{A})}$. Therefore, $e^{t(\omega_0(S))} = r(e^{t\mathcal{A}}) = e^{ts(\mathcal{A})}$, from which we can conclude that $s(A) \leq \omega_0(S)$, with equality if and only if $\mathcal{A}$ is bounded [64].

These spectral bounds will aid us in our quest to characterize steady-state solutions of the multi-structured model. This property has been demonstrated for the age-structured model in [33], and we conclude this section with a mathematical formulation of this problem wherein we seek a rank-one operator $\mathbf{P} \in \mathcal{L}(U, U_\lambda)$, the space of bounded linear operators from U to U_λ, where U_λ is an eigenspace of $\mathcal{A}$ corresponding to eigenvalue λ, such that

$$e^{-\lambda t}S(t) - \mathbf{P}$$

goes to zero exponentially in operator norm as $t \to \infty$ [65]. We are guaranteed the existence of such a projection if the following lemma (from [33]) is satisfied.

Lemma 4. *If λ is the positive, strictly dominant, simple, and real eigenvalue of the generator $\mathcal{A}$ of a strongly continuous semigroup $S(t)$, then there exists a rank-one operator $\mathbf{P}$ in the Banach space $\mathcal{L}(U, U_\lambda)$ such that the range of $\mathbf{P} = \ker(\mathcal{A} - \lambda I)$, a one-dimensional invariant subspace.*

Then there exist positive constants M and δ such that,

$$||e^{-\lambda t}S(t) - \mathbf{P}||_B \leq Me^{-\delta t}. \tag{4.2}$$

4.4 Semigroup Solution and ACP for the Multi-Structured Model

The solution given in (3.7) forms a strongly-continuous semigroup of linear operators $\{S(t)\}_{t\geq 0}$ where,

$$n(t,a,\bar{\mathbf{x}}) = (S(t)\phi)(a,\bar{\mathbf{x}}) = \begin{cases} \phi(a-t,\bar{\mathbf{X}}(-t,\bar{\mathbf{x}}))\Pi(t)J(t) & \text{for } t < a \\ n(t-a,0,\bar{\mathbf{X}}(-a,\bar{\mathbf{x}}))\Pi(a)J(a) & \text{for } t > a. \end{cases} \tag{4.3}$$

Lemma 5. *$\{S(t)\}$ is a strongly continuous semigroup on U.*

Proof. Provided in the appendix. □

While $\{S(t)\}_{t\geq 0}$ has several convenient properties by virtue of being a strongly-continuous semigroup, such as exponential boundedness, in order to make use of them, we must show that $\{S(t)\}_{t\geq 0}$ is *generated* by the linear operator associated with the model (3.4). The linear operator $\mathcal{A}$ associated with the PDE in (3.4) is,

$$\mathcal{A}\phi = -\left[\frac{\partial\phi}{\partial a} + \sum_{i=1}^{k} v_i \frac{\partial\phi}{\partial x_i} + \phi\sum_{i=1}^{k}\frac{\partial v_i}{\partial x_i} + \mu\phi\right]. \tag{4.4}$$

Through this operator, the PDE model may be recast as the Abstract Cauchy Problem in the Banach space $U = L^1(\mathbb{R}_+ \times \Omega)$, for $n(t,\cdot,\cdot)$:

$$\frac{dn(t)}{dt} = \mathcal{A}n(t), \quad n(0) = \phi. \tag{4.5}$$

Furthermore, we have proven (in Appendix E) that $\mathcal{A}$ is the infinitesimal generator of $\{S(t)\}_{t\geq 0}$ by showing that

$$\mathcal{A}\phi = \lim_{t\searrow 0}\frac{1}{t}(S(t)\phi - \phi)$$

is satisfied for every ϕ in the domain of $\mathcal{A}$, $\mathcal{D}(\mathcal{A})$ [31]. The Well-Posedness Theorem then guarantees that the ACP (4.5) is well-posed, and therefore $n(t,\cdot,\cdot) = S(t)\phi$ is the unique classical solution for $\phi \in \mathcal{D}(\mathcal{A})$.

4.5 The domain of the generator

The definition of the semigroup $S(t)$ and its generator $\mathcal{A}$ are incomplete without a definition of the domain, $\mathcal{D}(\mathcal{A})$. In the most general sense, the domain of a semigroup is a Banach space, or subset of a Banach space, where its generator is defined [32]. For this problem, $\mathcal{D}(\mathcal{A})$, is the subset of all ϕ in the Banach space $L^1(\mathbb{R}_+ \times \Omega)$ satisfying the following two properties:

(1) The boundary conditions must match. This means

$$\lim_{t\to 0^+} \frac{1}{t}\int_0^t \int_\Omega |\phi(a,\bar{\mathbf{x}}) - \hat{B}(0,\bar{\mathbf{x}})| d\bar{\mathbf{x}} da = 0$$

where $\hat{B}(t,\bar{\mathbf{x}}) = \displaystyle\int_0^\infty \int_\Omega \beta(a,\bar{\mathbf{y}},\bar{\mathbf{x}}) S(t) u(a,\bar{\mathbf{y}}) d\bar{\mathbf{y}} da.$

(2) The derivative must remain in the domain. This means that there exists some $\phi' \in L^1(\mathbb{R}_+ \times \Omega)$ such that for every $\tau \in \mathbb{R}$,

$$\phi(a-\tau, \bar{\mathbf{G}}^{-1}(\bar{\mathbf{G}}(\bar{\mathbf{x}}) - \tau)) - \phi(a,\bar{\mathbf{x}}) = \int_0^\tau \phi'(a-s, \bar{\mathbf{G}}^{-1}(\bar{\mathbf{G}}(\bar{\mathbf{x}}) - s)) ds$$

where $\phi(a-\tau, \bar{\mathbf{G}}^{-1}(\bar{\mathbf{G}}(\bar{\mathbf{x}}) - \tau))$ is defined to be zero on $[0, -\tau) \times \Omega$ if $\tau < 0$. If this is satisfied, then the directional derivative

$$D_{(1,\bar{\mathbf{v}})}\phi(a,\bar{\mathbf{x}}) = \lim_{\tau\to 0} \frac{1}{\tau}[\phi(a-\tau, \bar{\mathbf{G}}^{-1}(\bar{\mathbf{G}}(\bar{\mathbf{x}}) - \tau)) - \phi(a,\bar{\mathbf{x}})]$$

exists almost everywhere and is equal to $\phi'(a,\bar{\mathbf{x}})$

Under these conditions, we can restrict our domain to the Sobolev space $W^{1,1}(\mathbb{R}_+ \times \Omega)$, giving us the correct balance of regularity and integrability [42].

4.6 Reproduction as a semigroup perturbation

We have shown that the operator $\mathcal{A}$ generates the strongly continuous semigroup $S(t)$. A perturbation to the generator of a semigroup by a bounded linear operator produces

another generator of a strongly continuous semigroup [52]. If cells entering the population at the $a = 0$ boundary are conceived of as an input or impulse $m(t)$ fed into the system by the bounded linear operator $\mathcal{C}$, this acts as a perturbation to $\mathcal{A}$, changing our original abstract Cauchy problem to,

$$\frac{dn(t)}{dt} = \mathcal{A}n(t) + \mathcal{C}m(t). \tag{4.6}$$

However, specifying the generator of the perturbed semigroup is likely to be exceedingly difficult. Instead, we apply the variation of constants formula to get an integral equation for $n(t)$,

$$n(t) = S(t)\phi + \int_0^t S(t-s)\mathcal{C}m(s)ds,$$

and seek to characterize conditions on ϕ and m which make n differentiable.

By defining the system input cumulatively as $F(t) = \int_0^t \mathcal{C}m(s)ds$, the above integral equation can be expressed as the Stieltjes integral[1] ,

$$n(t) = S(t)\phi + \int_0^t S(t-s)F(ds). \tag{4.7}$$

Alternatively, the cumulative input to the system can be defined by a family of operators $V_0(t) = \int_0^t S(s)\mathcal{C}ds$, which form a *step response* for S, and the same expression for n becomes the Stieltjes integral,

$$n(t) = S(t)\phi + \int_0^t V_0(ds)m(t-s). \tag{4.8}$$

The interpretation of the step response is the same as in the ordinary differential equation setting. For example, take the suspension mechanism of a car to be the system, and rolling it off a curb to be the input. The step response of the suspension is the frequency and

[1] A Stieltjes integral,

$$\int_0^t W(ds)V(s)$$

in a Banach space is defined as the limit of the sums

$$\sum_{j=0}^{n}(U(r_{j+1}) - U(r_j))V(s_j), \quad s_j \in [r_j, r_{j+1}]$$

as the partition $0 = r_0 < \cdots < r_{n+1} = t$ becomes finer and finer.

amplitude with which the car wobbles in response. With this in hand, one can evaluate the car's performance on a variety of road conditions by convolving the response with the input function describing the surface of a particular road.

If the initial state of a system is at rest at the origin, $\phi = 0$, and receives an input, or an external force is applied in the form of a step function

$$m(t) = \begin{cases} 0 & t < 0 \\ \gamma & t \geq 0, \end{cases}$$

the time evolution of the system is given by $V_0(t)\gamma$. That is to say, convolution of an input with the step response determines the how the system will behave as a result.

As the rate of cell loss due to division is required to match the birth rate of new cells in our PDE model formulation, we account for this type of feedback mechanism by equating input to output. Setting $n(t) = m(t)$ in the variation-of-constants formula (4.8), and recognizing that $n(t) = T(t)\phi$, the perturbed semigroup, leads to a system of equations for $T(t)$ in terms of its associated step response $V(t)$, which inherits the step response properties of $V_0(t)$

$$T(t) = S(t) + \int_0^t V(ds)S(t-s) \tag{4.9}$$

$$V(t) = V_0(t) + \int_0^t V(t-s)V_0(ds). \tag{4.10}$$

Accordingly, a step response V_0 must satisfy the relationship,

$$V_0(t+s) - V_0(t) = S(t)V_0(s),$$

where the right hand side says that the state of the system at time s is $V_0(s)$ which S advances to $S(t)V_0(s)$ over the time interval s to $t+s$; the state of the system at time $t+s$ in response to an input over the whole time interval $[0, t+s)$, subtracting $V_0(t)$ on the left makes the change equivalent over the interval $[s, t+s)$.

Asymptotic behavior of the semigroup T is determined by its generator $\mathcal{A}+\mathcal{C}$. However, without access to this operator, we instead analyze spectral properties of $\mathcal{A}$ through its

resolvent operator $R(\lambda, \mathcal{A}) = (\lambda I - \mathcal{A})^{-1}$ and the step response V_0. The following theorem gives the relationship between a strongly continuous semigroup and the resolvent operator of its generator [52].

Theorem 6. *Let $T = \{T(t)\}_{t\geq 0}$ be a strongly continuous family of bounded linear operators. Then the following are equivalent.*

(1) T is a strongly continuous semigroup.

(2) There exists $s_0 \in \mathbb{R}_+$ such that the Laplace transform $\int_0^\infty e^{-\lambda t} T(t)x dt$ of $t \to T(t)x$ exists for all $\lambda > \lambda_0$ and x in the Banach space X, and there exists a linear operator $(\mathcal{A}, \mathcal{D}(\mathcal{A}))$ such that $(\lambda_0, \infty) \subset \rho(\mathcal{A})$ and, for all $x \in X$ and $\lambda > \lambda_0$,

$$\mathcal{R}(\lambda, \mathcal{A})x = \int_0^\infty e^{-\lambda t} T(t)x dt.$$

where $\mathcal{R}(\lambda, \mathcal{A}) = (\mathcal{A} - \lambda I)^{-1}$ is the resolvent operator of the generator of the semigroup $T(t)$.

Defining $V(t)x = \int_0^t S(r)x dr$, we recognize the first integral in (4.9) as a Stieltjes convolution integral defined,

$$(S * f) = \int_0^t V(ds) f(t-s).$$

Taking Laplace transforms,

$$\mathcal{L}(f(t)) = \hat{f}(\lambda) = \int_0^\infty e^{-\lambda t} f(t) dt,$$

of the integrals in (4.9) produces,

$$\begin{aligned}
&\mathcal{L}(T(t)) = \mathcal{L}(S(t)) + \int_0^t V(ds)S(t-s)) \Rightarrow \mathcal{R}(\lambda, \mathcal{A}+\mathcal{C}) = \mathcal{R}(\lambda, \mathcal{A}) + \hat{V}(\lambda)\mathcal{R}(\lambda, \mathcal{A}) \\
&\mathcal{L}(V(t)) = \mathcal{L}(V_0(t) + \int_0^t V(t-s)V_0(ds)) \Rightarrow \hat{V}(\lambda) = \hat{V}_0(\lambda) + \hat{V}(\lambda)\hat{V}_0(\lambda) \\
&\qquad \Rightarrow \mathcal{R}(\lambda, \mathcal{A}+\mathcal{C}) = (I - \hat{V}_0(\lambda))^{-1}\mathcal{R}(\lambda, \mathcal{A})
\end{aligned} \tag{4.11}$$

Singularities of $\mathcal{R}(\lambda, \mathcal{A}+\mathcal{C})$ are eigenvalues of the generator of the perturbed semigroup $T(t)$. The Hille-Yosida Theorem says that this eigenvalue λ_0 is of multiplicity 1 and by Theorem 4.5, we see that this eigenvalue is the spectral bound of the operator $\mathcal{A}+\mathcal{C}$. Furthermore, Lemma 4.3 above states that the corresponding eigenfunction ψ_{λ_0} spans the eigenspace $\ker((\mathcal{A}+\mathcal{C})-\lambda I)$, an invariant subspace. Putting this all together, we see that if

$$(\mathcal{A}+\mathcal{C})\psi_\lambda = \lambda\psi_\lambda$$

has a solution λ_0, a singularity of the corresponding resolvent operator, then the eigenfunction ψ_λ is a rank-one projection to an invariant subspace of our state-space Ω, and therefore the asymptotic behavior of the population is determined by this eigenpair in that,

$$n(t,\cdot,\cdot) = T(t)\phi \sim e^{\lambda_0 t}\psi_{\lambda_0}. \tag{4.12}$$

From (4.11), it is clear that singular points of $\mathcal{R}(\lambda, \mathcal{A}+\mathcal{C})$, meaning eigenvalues of $(\mathcal{A}+\mathcal{C})$, are values of λ for which $\hat{V}_0(\lambda)$ has an eigenvalue equal to one. Identifying the operator $V_0(t)$, and taking its Laplace transform leads to the characteristic equation for λ_0.

4.7 Solving the characteristic equation for our model

For the multi-structured model, the semigroup $S(t)$ and its corresponding step response $V_0(t)$ are defined by,

$$\begin{aligned}(S(t)\phi)(a,\bar{\mathbf{x}}) &= \phi(a-t, \bar{\mathbf{X}}(-a,\bar{\mathbf{x}}))\Pi(t)J(t)\\ (V_0(t)\phi)(a,\bar{\mathbf{x}}) &= \Pi(a)J(a)\int_0^t \left(\int_{\Omega_m} \phi(a+s,\bar{\mathbf{y}})\beta_0(a+s,\bar{\mathbf{x}})(d\bar{\mathbf{y}})\right) L(a+ds,\bar{\mathbf{x}}).\end{aligned} \tag{4.13}$$

In the expression for the step response V_0 above, $\beta_0(a,\bar{\mathbf{x}})(d\bar{\mathbf{y}})$ is a probability measure on Ω. Consider for a moment cell length to be the only structure variable, then $\Omega_m = (\frac{x_M}{2}, x_M]$, and the interval can be partitioned more and more finely, as in $\Omega_m = \frac{x_M}{2} = r_0 < r_1 < \cdots < r_{j-1} < r_j < -r_{j+1} < \cdots < r_N = x_M]$. Within each interval of the partition, $\beta_0(a,x_1)(r_{j+1}) - \beta_0(a,x_1)(r_j)$ is the probability that a newborn cell will have length x_1, given

that its mother was of length $y_1 \in [r_j, r_{j+1}]$ and age a at division. With all of the structure variables included, these partitions become subsets $\omega \subset \Omega$. Integrating this probability measure against a distribution over all of Ω, as in $\int_{\Omega_m} \phi(a, \bar{\mathbf{y}})\beta_0(a, \bar{\mathbf{x}})(d\bar{\mathbf{y}})$ counts of the number of individuals of state $\bar{\mathbf{y}}$ times the probability that they will divide.

The functional $L(da, \bar{\mathbf{x}})$ is also defined as a measure on Ω and represents the *cumulative* expected number of cells of state $\bar{\mathbf{x}}$, produced by a mother cell of age $a \in [a, a + da]$, thus

$$L(da, \bar{\mathbf{x}}) = \int_a^{a+da} \int_{\Omega_m} \beta(s, \bar{\mathbf{y}}, \bar{\mathbf{x}}) d\bar{\mathbf{x}} ds = \int_a^{a+da} 2^{k+1}\beta_1(s)\chi_{\{\bar{\mathbf{y}} \in \Omega_m\}} ds.$$

The expression for the step response $V_0(t)$ is saying that, given the *input*, the distribution $\phi(a, \bar{\mathbf{x}})$ of cells at time t, the system response is the number of cells of age zero and state $\bar{\mathbf{x}}$ produced within the infinitesimal time interval $[t, t + dt]$.

The Laplace transform of the step response is,

$$\begin{aligned}
\mathcal{L}((V_0(t)\phi)(a, \bar{\mathbf{x}})) &= \int_0^\infty e^{-\lambda\tau} V_0(d\tau)(a, \bar{\mathbf{x}}) \\
&= \Pi(a)J(a) \int_0^\infty e^{-\lambda\tau} \left(\int_{\Omega_m} \phi(a + s, \bar{\mathbf{y}})\beta_0(a + s, \bar{\mathbf{x}})(d\bar{\mathbf{y}}) \right) L(a + d\tau, \bar{\mathbf{x}}) \\
&= \Pi(a)J(a) \int_0^\infty e^{-\lambda\tau} \left(2^{k+1}\beta_1(a + s)\phi(a + s, 2\bar{\mathbf{x}}) \right) L(a + d\tau, \bar{\mathbf{x}}) \\
&\text{Let } \sigma = a + \tau \\
&= \Pi(a)J(a)e^{\lambda a} \int_a^\infty e^{-\lambda\sigma} \left(2^{k+1}\beta_1(\sigma)\phi(\sigma, 2\bar{\mathbf{x}}) \right) 2^{k+1}\beta_1(\sigma) d\sigma \\
&= \Pi(a)J(a)e^{\lambda a} \int_a^\infty e^{-\lambda\sigma} 2^{2k+2} (\beta_1(\sigma))^2 \phi(\sigma, 2\bar{\mathbf{x}}) d\sigma
\end{aligned} \tag{4.14}$$

Finally, we see that if $\hat{V}_0(\lambda)$ is to have an eigenvalue of one, we need to find λ such that

$$(\hat{V}_0(\lambda)\phi)(a, \bar{\mathbf{x}}) = \Pi(a)J(a)e^{\lambda a} \int_a^\infty e^{-\lambda\sigma} 2^{2k+2} (\beta_1(\sigma))^2 \phi(\sigma, 2\bar{\mathbf{x}}) d\sigma = \phi(a, \bar{\mathbf{x}}) \tag{4.15}$$

However, by absorbing the Jacobian into the integral to perform the coordinate transformation $\bar{\mathbf{x}} \to \bar{\mathbf{X}}(-a, \bar{\mathbf{x}})$ and defining an operator $K(\lambda) : C(\Omega) \to C(\Omega)$ by

$$(K(\lambda)\psi)(\bar{\mathbf{x}}) = \int_0^\infty e^{-\lambda\sigma} 2^{2k+2} (\beta_1(\sigma))^2 \psi(\bar{\mathbf{X}}(-a, 2\bar{\mathbf{x}})) d\sigma$$

we derive an equivalent eigenproblem,

$$(K(\lambda)\psi)(\bar{\mathbf{x}}) = \psi(\bar{\mathbf{x}}) = \int_0^\infty e^{-\lambda\sigma} \left(2^{k+1}\beta_1(\sigma)\right)^2 \psi(\bar{\mathbf{X}}(-a, 2\bar{\mathbf{x}}))d\sigma \tag{4.16}$$

for the eigenvalue λ and corresponding eigenfunction $\psi(\bar{\mathbf{x}})$, since $\hat{V}_0(\lambda)$ will have an eigenvalue of one whenever $K(\lambda)$ does. We will return to this eigenproblem for the perturbed semigroup in comparison with the eigenproblem derived from the renewal equation.

In summary, solutions to (6.1) lead to an asymptotic solution to the multi-structured model (3.4) with growth rate λ and state-space distribution $\psi(\bar{\mathbf{x}})$. We derived this equation by perturbing the generator of the semigroup solution (4.3) with a bounded linear operator. As is typical in this scenario, we do not have access to the perturbed generator, and instead we relate the associated perturbed semigroup $T(t)$ to our original semigroup solution $S(t)$ through a step-response operator. Spectral properties of the perturbed operator determine the long-term behavior of the perturbed semigroup, and Theorem 6 provides a connection to the spectrum of the perturbed generator as its resolvent operator is the Laplace transform of the perturbed semigroup.

This leads to an expression for the resolvent operator of the perturbed generator, from which we can access its spectrum as singularities of the resolvent are necessarily in the spectrum. It is clear from this expression that an eigenvalue of the perturbed generator is the value of λ for which the Laplace transform of the step-response operator has itself an eigenvalue of 1. By solving this characteristic equation we arrive at the eigenproblem (6.1) above.

Together, the Hille-Yosida Theorem and the Perron-Frobenius Theorem for positive semigroups assert that the eigenvalue λ is the spectral bound of the perturbed generator. By applying the Spectral Mapping Theorem, we see that λ is also the uniform growth bound of the perturbed semigroup $T(t)$. Furthermore, the corresponding eigenfunction $\psi(\bar{\mathbf{x}})$, spans the eigenspace of the perturbed generator corresponding to λ, the kernel of $(\mathcal{A}+\mathcal{C})-\lambda I$, and is therefore the projection $\mathbf{P}$ described in Lemma 4 describing the steady-state distribution

in state-space.

Chapter 5

Renewal Equation Approach

In the previous chapter, we perturbed the generator of the semigroup solution to the multi-structured model (3.4), and arrived at an eigenequation for which the eigenvalue λ and corresponding eigenfunction $\psi(\bar{\mathbf{x}})$ dictate the asymptotic behavior of the population as $t \to \infty$. In this chapter, we will analyze an abstract renewal equation derived from the renewal equation at the age $a = 0$ boundary found in Chapter 3, and arrive at a similar eigenfunction (to be solved in Chapter 6) with solutions λ and $\psi(\bar{\mathbf{x}})$ to determine again the asymptotic behavior of the population as $t \to \infty$.

5.1 Reduction to an abstract renewal equation

In this section, an alternative approach to resolving cell renewal at the age $a = 0$ boundary is presented. The integral equation for $B(t, \bar{\mathbf{x}})$ is repeated here from (3.8).

$$\begin{aligned} B(t,\bar{\mathbf{x}}) &= \int_0^t \int_\Omega \beta(a,\bar{\mathbf{y}},\bar{\mathbf{x}}) B(t-a, \bar{\mathbf{Y}}(-a,\bar{\mathbf{y}})) \exp\left[-\int_0^a \mu(\sigma, \bar{\mathbf{Y}}(\sigma-a,\bar{\mathbf{y}}))d\sigma\right] J(a) d\bar{\mathbf{y}} da \\ &+ \int_t^\infty \int_\Omega \beta(a,\bar{\mathbf{y}},\bar{\mathbf{x}}) \phi(a-t, \bar{\mathbf{Y}}(-t,\bar{\mathbf{y}})) \exp\left[-\int_0^t \mu(a+\sigma-t, \bar{\mathbf{Y}}(\sigma-t,\bar{\mathbf{y}}))d\sigma\right] J(t) d\bar{\mathbf{y}} da \\ &= K(B)(t,\bar{\mathbf{x}}) + \Phi(t,\bar{\mathbf{x}}) \end{aligned} \tag{5.1}$$

Identifying $\Phi(t, \bar{\mathbf{x}})$ and $B(t, \bar{\mathbf{x}})$ with their respective mappings $t \to \Phi(t, \cdot)$ and $t \to$

$B(t,\cdot)$, we can write (3.8) as the abstract renewal equation,

$$B(t) = \Phi(t) + \int_0^t K(a)B(t-a)da. \tag{5.2}$$

where, for each *fixed* t, $B(t)$ and $\Phi(t)$ are operators in $L_1(\Omega)$ in that $B(t,\bar{\mathbf{x}}) = (B(t))(\bar{\mathbf{x}})$, and similarly for Φ.

And similarly, for each *fixed* t, $K(t)$ defines a bounded linear operator from $L_1(\Omega) \to L_1(\Omega)$. Let $\psi(\bar{\mathbf{x}})$ be an L_1-function on Ω. Then, $(K(t)\psi)(\bar{\mathbf{x}})$ maps $\psi(\bar{\mathbf{x}}) \in L_1(\Omega)$ to another function in $L_1(\Omega)$ through multiplication and translation by the kernel $\mathcal{K}(t,\bar{\mathbf{x}})$, where,

$$\begin{aligned}
K(B)(t,\bar{\mathbf{x}}) &= \int_0^t \int_\Omega \beta(a,\bar{\mathbf{y}},\bar{\mathbf{x}})B(t-a,\bar{\mathbf{Y}}(-a,\bar{\mathbf{y}}))\Pi(a;a,\bar{\mathbf{x}})J(a;a,\bar{\mathbf{x}})d\bar{\mathbf{y}}da \\
&= \int_0^t \int_\Omega \beta_1(a)\chi_{\{\bar{\mathbf{y}}\in\Omega_m\}}\delta(\bar{\mathbf{x}} - \frac{1}{2}\bar{\mathbf{y}})B(t-a,\bar{\mathbf{Y}}(-a,\bar{\mathbf{y}}))\Pi(a;a,\bar{\mathbf{x}})J(a;a,\bar{\mathbf{x}})d\bar{\mathbf{y}}da \\
&= \int_0^t \beta_1(a)\chi_{\{\bar{\mathbf{y}}\in\Omega_m\}}B(t-a,\bar{\mathbf{Y}}(-a,2\bar{\mathbf{y}}))\Pi(a;a,2\bar{\mathbf{x}})J(a;a,2\bar{\mathbf{x}})da \\
&= \int_0^t \mathcal{K}(a,2\bar{\mathbf{x}})B(t-a,\bar{\mathbf{Y}}(-a,2\bar{\mathbf{y}}))da.
\end{aligned} \tag{5.3}$$

We define $\mathcal{K}(a,\bar{\mathbf{x}})$ by, $\mathcal{K}(a,\bar{\mathbf{x}}) = \beta_1(a)\Pi(a;a,\bar{\mathbf{x}})J(a;a,\bar{\mathbf{x}})\chi_{\{\bar{\mathbf{y}}\in\Omega_m\}}$, and see that,

$$(K(t)\Psi)(\bar{\mathbf{x}}) = \mathcal{K}(t,2\bar{\mathbf{x}})\Psi(\bar{\mathbf{X}}(-t,2\bar{\mathbf{x}})) \in L_1(\Omega).$$

5.2 Domain and Range of Operators

In this section, we will discuss the continuity requirements and restrictions for each operator. The renewal equation is composed of three operators, $B(t,\bar{\mathbf{x}})$, $\Phi(t,\bar{\mathbf{x}})$, and $\mathcal{K}(a,\bar{\mathbf{x}})$, which functions as an integral kernel integrated against $B(a,\bar{\mathbf{x}})$ with respect to a on $[0,t]$. Each of these continuous functions is non-negative, has compact support, and acts on the space $\mathbb{R}_+ \times \Omega$.

Lemma 7. *For each $t \in [0,T]$, there is a unique, continuous mapping from the interval $[0,T]$ into $L_1(\Omega)$, such that $\Phi(t,\cdot)$ and $B(t,\cdot)$ satisfy the integral equation (3.8).*

Proof. $\Phi(t, \bar{\mathbf{x}})$ is obtained by integrating the initial condition $\phi(a, \bar{\mathbf{x}})$ along characteristic curves for $a \in (0, \infty)$. Since ϕ is assumed to be a Lipschitz continuous, compactly supported function in $L_1(\mathbb{R}_+ \times \Omega)$, integration over all ages a produces a continuous function in $L_1(\Omega)$. In this way, for each fixed $t \in [0, T]$, there exists a unique, continuous mapping $t \to \Phi(t, \bar{\mathbf{x}})$ from the interval $[0, T] \to L_1(\Omega)$, with $\Phi(t, \cdot)$ satisfying the integral equation (3.8).
The result for B was proven in Theorem 3.1. □

Further, since $G(2x_1)$ is the time required for the smallest possible cell to reach a length of $2x_1$, we consider $\Phi(t, \bar{\mathbf{x}}) = 0$ if $t \geq G(2x_1)$, because any cell present at time $t = 0$ will necessarily have surpassed this length, and there will be no contribution of new cells of length x_1.

And finally, $\mathcal{K}(a, \bar{\mathbf{x}})$ can be thought of as an integral kernel, continuous in both a and $\bar{\mathbf{x}}$. Continuity of $\mathcal{K}$ guarantees the existence of a unique, continuous L_1-function B that is the solution to (3.8). $\mathcal{K}(a, 2\bar{\mathbf{x}}) = 0$ if $\bar{\mathbf{x}} \notin \Omega_m$, as these cells are too small to divide, and $\mathcal{K}(a, 2\bar{\mathbf{x}}) = 0$ if $a \geq G(2x_1)$ as, similar to Φ, these cells are older than the time it takes to grow to size $2x_1$, and would therefore be too large to produce cells of size x_1.

5.2.1 Laplace Transform

The Laplace transform of a function $f(t)$ is denoted and defined

$$\hat{f}(\lambda) = \int_0^\infty e^{-\lambda t} f(t) dt.$$

Taking the Laplace transform of both sides of the abstract renewal equation,

$$B(t) = \Phi(t) + \int_0^t K(a) B(t - a) da \tag{5.4}$$

yields,

$$\hat{B}(\lambda) = \hat{\Phi}(\lambda) + \hat{K}(\lambda)\hat{B}(\lambda) \quad \Rightarrow \quad \hat{B}(\lambda) = (I - \hat{K}(\lambda))^{-1}\hat{\Phi}(\lambda). \tag{5.5}$$

The solution $B(t)$ is then the inverse Laplace transform of $\hat{B}(\lambda)$,

$$B(t) = \mathcal{L}^{-1}\{\hat{B}(\lambda)\} = \frac{1}{2\pi i} \int_{c-i\infty}^{c+i\infty} e^{\lambda t} (I - \hat{K}(\lambda))^{-1} \hat{\Phi}(\lambda) d\lambda.$$

Cauchy's Residue Theorem says that the solution to this complex integral is the sum over the residues of $\hat{B}(\lambda)$ at each pole. We will show that singularities of $\hat{B}(\lambda)$ only exist when $(I - \hat{K}(\lambda))^{-1}$ is singular, and that this a simple pole defined for a unique value of λ.

We have shown previously that the solution to the model (3.4) generates a semigroup of linear operators which, one of the properties this endows $K(t)$ and $\Phi(t)$ with, is that they are exponentially bounded by a bound on the probability of cell loss. Let

$$\mu_\infty = \lim_{\sigma \to \infty} \mu(a + \sigma, \bar{\mathbf{X}}(\sigma, \bar{\mathbf{x}})) \leq d + 1 < \infty.$$

Then, $||\Phi(t)|| \leq M_1 e^{-\mu_\infty t}$, and $||K(t)\psi|| \leq ||\psi|| M_2 e^{-\mu_\infty t}$. Therefore, $\hat{K}(\lambda)$ and $\hat{\Phi}(\lambda)$ are both analytic where they are defined, that is for all λ in the right-half plane

$$\Lambda = \{\lambda \in \mathbb{C} | Re(\lambda) > -\mu_\infty\}.$$

The operators are not defined for $Re(\lambda) < -\mu_\infty$ as the exponent in the Laplace transform would become positive forcing the integral to diverge.

As the operators $\hat{K}(\lambda)$ and $\hat{\Phi}(\lambda)$ are both analytic in Λ, the only singularities will arise when $1 \in \sigma(\hat{K}(\lambda))$, the spectrum of the Laplace transform of $K(t)$. Therefore, the long-term behavior of $B(t)$ will be determined by the element $\lambda \in \Lambda$ with the largest real part such that $I - \hat{K}(\lambda)$ is singular.

Here we present a series of arguments as laid out in Heijman's analysis of an age and size structured model appearing in [47]. These results hold for the multi-structured model and together assert that there is one dominant eigenvalue λ_0, equal to the spectral radius of the semigroup $S(t)$, thus determining the long-term behavior of the system along with the corresponding eigenfunction ψ_{λ_0}.

Lemma 8. *For all $\lambda \in \Lambda$, $\hat{K}(\lambda)$ is compact.*

Lemma 9. *The function $\lambda \to (I - \hat{K}(\lambda))^{-1}$ is meromorphic in Λ.*

If the mapping from λ to the operator $(I - \hat{K}(\lambda))^{-1}$ is meromorphic, the set

$$\Sigma = \{\lambda \in \Lambda | 1 \in \sigma(\hat{K}(\lambda))\}$$

is a discrete set whose elements are poles of $(I - \hat{K}(\lambda))^{-1}$ of finite order.

Lemma 10. *If ψ is an eigenfunction of $\hat{K}(\lambda)$, then $\psi(\bar{\mathbf{x}}) = 0$ for $\bar{\mathbf{x}} \notin \Omega_m$.*

From this lemma, we see that repeated applications of $\hat{K}(\lambda)$ are ultimately restricted to the subspace of $L_1(\Omega)$ spanned by ψ, and therefore, $\hat{K}(\lambda)$ restricted to this subspace is *non-supporting*. If $\hat{K}(\lambda)$ is non-supporting, then the spectral radius $r = r(\hat{K}(\lambda))$, is a pole of the resolvent, $(\lambda I - \hat{K}(\lambda))^{-1}$, and an algebraically simple eigenvalue of $\hat{K}(\lambda)$.

Lemma 11. *The corresponding eigenvector $\psi_\lambda(\bar{\mathbf{x}}) > 0 \; \forall \; \bar{\mathbf{x}} \in \Omega_m$.*

Lemma 12. *There is a unique $\lambda_0 \in \Lambda \cap \mathbb{R}$ such that $r = 1$, and therefore $\lambda_0 \in \Sigma$.*

Lemma 13. *And finally, all other $\lambda \in \Sigma$ have $Re(\lambda) < \lambda_0$.*

That is, λ_0 is the unique eigenvalue which makes the spectral radius of $\hat{K}(\lambda)$ equal to one, and all other eigenvalues in the set Σ are separated from λ_0 by some positive horizontal distance.

Therefore, solving the abstract renewal equation reduces to the characteristic equation for $\hat{K}(\lambda)$, for which we must find the value of λ, and its corresponding eigenvector ψ_λ, such that $(\hat{K}(\lambda)\psi)(\bar{\mathbf{x}}) = 1\psi(\bar{\mathbf{x}}) = \psi(\bar{\mathbf{x}})$.

5.3 Solution to the eigenproblem

We seek a solution to the renewal equation wherein the contribution from the initial condition becomes negligible on a large time frame, and the behavior of $B(t, \bar{\mathbf{x}})$ can be described in terms of its dominant eigenvalue and corresponding eigenfunction, as in

$$B(t, \bar{\mathbf{x}}) = K(B)(t, \bar{\mathbf{x}}) + \Phi(t, \bar{\mathbf{x}}) \sim e^{\lambda t}\psi(\bar{\mathbf{x}}),$$

as $t \to \infty$. We have shown in the previous section that λ and ψ are the unique solutions to the characteristic equation for $\hat{K}(\lambda)$. That is,

$$\begin{aligned}(K(t)e^{\lambda t}\psi)(\bar{\mathbf{x}}) = e^{\lambda t}\psi(\bar{\mathbf{x}}) &= \int_0^t \mathcal{K}(a, 2\bar{\mathbf{x}})B(t-a, \bar{\mathbf{X}}(-a, 2\bar{\mathbf{x}}))da \\ &= e^{\lambda t}\psi(\bar{\mathbf{x}}) = \int_0^t e^{\lambda(t-a)}\mathcal{K}(a, 2\bar{\mathbf{x}})\psi(\bar{\mathbf{X}}(-a, 2\bar{\mathbf{x}}))da \\ &\Rightarrow \psi(\bar{\mathbf{x}}) = \int_0^t e^{-\lambda a}\mathcal{K}(a, 2\bar{\mathbf{x}})\psi(\bar{\mathbf{X}}(-a, 2\bar{\mathbf{x}}))da \\ \psi(\bar{\mathbf{x}}) &= \int_0^t e^{-\lambda a}\Pi(a)J(a)\beta_1(a)\psi(\bar{\mathbf{X}}(-a, 2\bar{\mathbf{x}}))da\end{aligned} \tag{5.6}$$

Here we have arrived at the eigenequation for λ and ψ. Solving this equation requires us to specify a division condition as well as conditions on the growth rate which we will complete in the following concluding chapter.

As in the previous chapter, we begin by casting our problem abstractly (Banach-space valued), and seek solutions in the form of linear operators acting on a Banach space. By taking Laplace transforms on either side of the abstract renewal equation (5.2), we find that the long-term behavior of $B(t)$ is determined by the value of λ such that the Laplace transform of $K(t)$ has itself eigenvalue 1. Properties of the unperturbed semigroup solution (4.3) guarantee that $K(t)$ is analytic and exponentially bounded, from which we show that the spectral radius of $\hat{K}(\lambda)$ is an algebraically simple eigenvalue equal to 1. This defines the characteristic equation we solve to arrive at the eigenequation for λ and $\psi(\bar{\mathbf{x}})$.

In the next chapter, we make assumptions and impose a division condition on our population so that we may solve the eigenequations derived from both the semigroup and renewal equation approaches, and determine the long-term behavior of the population.

Chapter 6

Summary of multi-structured modeling

In this chapter we will make some simplifying assumptions about cell growth and division in order to solve the eigenfunctions we have derived from the semigroup perturbation approach, and in the previous chapter, by solving the renewal equation. We conclude by comparing these solutions and discussing their interpretation.

6.1 Steady-state

At the end of Chapters 4 and 5, we concluded with the eigenproblem for the asymptotic solution to the renewal equation derived from semigroup perturbation and applying Laplace transforms to the renewal equation, respectively.

In order to complete these solutions, we must specify a division condition. For simplicity, will assume a constant growth rate α so that,

$$X_1(t, x_1) = x_1 e^{t\alpha},$$

and the Jacobian $J(t)$ reduces to

$$J(t) = e^{-t\alpha}.$$

As a condition for division, we will require a cell to double in length, so that if a cell is of size $\bar{\mathbf{x}}$ at birth, it will divide upon reaching size $2\bar{\mathbf{x}}$. Under this division condition, and with a constant growth rate, all cells will divide upon reaching the same age, a_*. Therefore, $\beta_1(a)$ becomes $\delta(a - a_*)$.

Now, we apply these conditions to the eigenproblems derived in Chapters 4 and 5.

6.1.1 Eigenproblem solution from semigroup perturbation

The eigenproblem for the Laplace transform of the step response operator $\hat{V}_0(\lambda)$ is equivalent to the eigenproblem defined through operator $K(\lambda) : C(\Omega) \to C(\Omega)$ where

$$(K(\lambda)\psi)(\bar{\mathbf{x}}) = \int_0^\infty e^{-\lambda\sigma} 2^{2k+2} (\beta_1(\sigma))^2 \psi(2\bar{\mathbf{x}}) d\sigma.$$

And the equivalent eigenproblem is,

$$(K(\lambda)\psi)(\bar{\mathbf{x}}) = \psi(\bar{\mathbf{x}}) = \int_0^\infty e^{-\lambda\sigma} \left(2^{k+1}\beta_1(\sigma)\right)^2 \psi(\bar{\mathbf{X}}(-a, 2\bar{\mathbf{x}})) d\sigma \tag{6.1}$$

Inserting our definition of $\beta_1(a)$ and $\delta(a - a_*)$, we find,

$$\begin{aligned} \psi(\bar{\mathbf{x}}) &= \int_0^\infty e^{-\lambda\sigma} \left(2^{k+1}\beta_1(\sigma)\right)^2 \psi(\bar{\mathbf{X}}(-a, \bar{\mathbf{x}})) d\sigma \\ &= \int_0^\infty e^{-\lambda\sigma} \left(2^{k+1}\delta(\sigma - a_*)\right)^2 \psi(\bar{\mathbf{X}}(-a, 2\bar{\mathbf{x}})) d\sigma \\ &= 2^{2k+2} e^{-\lambda a_*} \psi(\bar{\mathbf{X}}(-a_*, 2\bar{\mathbf{x}})) \end{aligned} \tag{6.2}$$

If all cells grow at a constant rate α, we find that the time it will take a cell to double in size is $a_* = \frac{1}{\alpha}\ln(2)$. Inserting this above, we find that λ must be equal to the growth rate α. Then the eigenfunction $\psi(\bar{\mathbf{x}}) = C\delta(\bar{\mathbf{x}})$ where $C = 2^{2k+1}$. This eigenfunction says that once a cell reaches age a_*, any state is a solution to the eigenequation as it will have reached the appropriate size for division, and divide to make a cell of state $\bar{\mathbf{x}}$.

Finally, we can express the long term behavior of the semigroup $T(t)$ as,

$$n(t, \cdot, \cdot) = T(t)\phi \sim e^{\lambda_0 t}\psi_{\lambda_0} = e^{\alpha t}\left(2^{2k+1}\delta(\bar{\mathbf{x}})\right).$$

6.1.2 Eigenproblem solution from renewal equation

Now, we will turn to the eigenequation we derived from the renewal equation in Chapter 5. We have,

$$\begin{aligned}\psi(\bar{\mathbf{x}}) &= \int_0^t e^{-\lambda a}\Pi(a)J(a)\beta_1(a)\psi(\bar{\mathbf{X}}(-a,2\bar{\mathbf{x}}))da \\ \psi(\bar{\mathbf{x}}) &= \int_0^t 2^{\frac{1}{\alpha}+1}e^{-a(d+1+\alpha+\lambda)}\psi(\bar{\mathbf{X}}(-a,2\bar{\mathbf{x}}))da \\ &= \int_0^t \left(2^{\frac{1}{\alpha}}e^{-a}\right)2e^{-a(d+\alpha+\lambda)}\psi(\bar{\mathbf{X}}(-a,2\bar{\mathbf{x}}))da\end{aligned} \tag{6.3}$$

The term in parenthesis is the contribution to the survival probability due to cell division,

$$\exp\left[-\int_0^a \mu(\sigma,\bar{\mathbf{Y}}(\sigma-a,\bar{\mathbf{y}}))d\sigma\right] = e^{-ad}\exp\left[-\int_0^a b(\sigma,\bar{\mathbf{Y}}(\sigma-a,\bar{\mathbf{y}}))d\sigma\right] = e^{-ad}2^{\frac{1}{\alpha}}e^{-a},$$

meaning, it gives the probability at each age that a cell of a given state will not divide. However, because we know that each cell must divide at the exact same age, $a_* = \frac{1}{\alpha}\ln 2$, we can change this probability to be zero everywhere and 1 (or infinite) upon reaching age a_*. That is to say, the probability of cell division a large t is entirely concentrated at a_* and so we can represent it with the Dirac delta function $\delta(a-a_*)$. Making this change in the above equation allows us to evaluate the integral and find a solution for the eigenvalue λ and it's corresponding eigenfunction ψ.

$$\begin{aligned}\psi(\bar{\mathbf{x}}) &= \int_0^t \left(2^{\frac{1}{\alpha}}e^{-a}\right)2e^{-a(d+\alpha+\lambda)}\psi(\bar{\mathbf{X}}(-a,2\bar{\mathbf{x}}))da \\ &= \int_0^t \delta(a-a_*)2e^{-a(d+\alpha+\lambda)}\psi(\bar{\mathbf{X}}(-a,2\bar{\mathbf{x}}))da \\ &= 2e^{-a_*(d+\alpha+\lambda)}\psi(\bar{\mathbf{X}}(-a_*,2\bar{\mathbf{x}}))\end{aligned} \tag{6.4}$$

The Jacobian term $e^{-a_*\alpha}$ must remain with the characteristic curve to avoid creating an imbalance as cells grow. The eigenfunction ψ will take the form of a δ function as it will act to "pick up" cells of the appropriate state, e.g., cells of length $2x_1$. However, since every cell divides upon doubling in size and reaching age a_*, every cell-state is a solution in that,

the characteristic curve on the right-hand-side describes a cell currently of length $2x_1$ that was of length x_1 at birth, a time a_* ago, exactly the cell required to produce the one on the left-hand-side. Therefore, $\psi(\bar{\mathbf{x}}) = C\delta(\bar{\mathbf{x}})$, where C is a constant. Since deaths are included in this model, the arbitrary constant C will absorb the constant probability of cell death. Finally, $\psi(\bar{\mathbf{x}}) = e^{-da_*}\delta(\bar{\mathbf{x}})$. Solving for λ here is equivalent to setting

$$2e^{-a_*\lambda} = 1 \Rightarrow \lambda = \frac{\ln 2}{a_*} = \alpha.$$

Therefore, after a short transient phase, we can characterize cell renewal for large values of t as

$$B(t, \bar{\mathbf{x}}) \sim e^{\lambda t}\psi(\bar{\mathbf{x}}) = e^{\alpha t}\left(e^{-a_* d}\delta(\bar{\mathbf{x}})\right)$$

In both cases, we find that the asymptotic growth rate is equal to the constant growth rate of cells, and that if all cells divide at the same age, the eigenfunction ψ reduces to a Dirac-delta function for which any cell of age a_* is a solution as these cells will necessarily have doubled in size. The eigenfunction solutions differ only by a constant, showing that from the two different approaches we presented, our results are consistent and predict the same asymptotic behavior.

Chapter 7

Conclusion

7.1 Comparison of solution

We have presented two different analyses and solution methods for resolving the asymptotic behavior of the population described by the multi-structured model, and shown that both methods arrive at the same conclusion. Following a short, transient phase, the system grows asymptotically according to,

$$n(t, a, \bar{\mathbf{x}}) \sim Ce^{\alpha t}\delta(\bar{\mathbf{x}})$$

as time grows toward infinity. The asymptotic solution says that, given an initial distribution, we will observe a wave-front like behavior wherein the initial cohort of cells will grow to double in size, and then reappear as cells of age zero at the exact same state that they and their mother cells had at birth.

7.2 Discussion

There is some debate as to whether this constitutes a true steady-state solution, or if it should instead be interpreted as a periodic solution (see Bell's 1967 conclusion [10], and Heijman's rebuttal [47]). Nevertheless, we have demonstrated that under some simple assumptions on cell growth and division, an asymptotic solution wherein evolution in time is separate from a predictable state-space behavior does exist for the multi-structured model.

This solution lays a framework for future investigation of structured population dynamics. For example, it has been proposed that a more accurate condition for cell division, which leads to convergence in cell length at birth, has cells grow by a constant amount before they divide, as opposed to reaching some set division length or doubling in size [18]. Under this assumption on division, and with a constant growth rate, we can similarly resolve the asymptotic behavior of our system by expressing the division age a_*, the time it takes to grow by a prescribed constant length ΔL, as a function of cell length at birth, $X_1(-a, x_1)$. We have that $G(x)$ is the time it takes to grow from the smallest possible size, x_m to size x, therefore a_* would be $a_* = G(X_1(-a, x_1) + \Delta L) - a$.

In future work, we will apply this model, and the methods used to find an asymptotic solution, to investigate the effect of aging on carboxysome productivity by changing the growth rate of cells to be carboxysome age-dependent. Changing the model in this way, or expanding it to include competition between cells, will introduce further complexity and nonlinearity to our model equations. However, the work presented in this dissertation will serve as the linearized model upon which analysis of the nonlinear extension would rely.

Bibliography

[1] Michael P Allen and Dominic J Tildesley. Computer simulation of liquids. Oxford university press, 2017.

[2] GEORGE E ANDREWS. One-parameter semigroups of positive operators, by w. arendt, a. grabosch, g. greiner, u. groh, hp lotz, u. moustakas, r. nagel, f. neubrander, and u. schlotterbeck. edited by r. nagel. lecture notes in mathematics, vol. 1184, springer-verlag, berlin, heidelberg, new york, tokyo, 1986, x 4-460 pp., isbn 3-540-16454-5, 1987.

[3] DV Annosov, S Kh Aranson, VI Arnold, IU Bronshtein, VZ Grines, and Yu S Ilyashenko. Ordinary differential equations and smooth dynamical systems, 1997.

[4] Ovide Arino. Some spectral properties for the asymptotic behavior of semigroups connected to population dynamics. SIAM review, 34(3):445–476, 1992.

[5] Ovide Arino. A survey of structured cell population dynamics. Acta biotheoretica, 43(1):3–25, 1995.

[6] Pierre Auger, Pierre Magal, and Shigui Ruan. Structured population models in biology and epidemiology, volume 1936. Springer, 2008.

[7] Albert Balows, Hans G Trüper, Martin Dworkin, Wim Harder, and Karl-Heinz Schleifer. The prokaryotes: a handbook on the biology of bacteria: ecophysiology, isolation, identification, applications. Springer Science & Business Media, 2013.

[8] Jacek Banasiak and Mirosław Lachowicz. Methods of small parameter in mathematical biology. Springer, 2014.

[9] H Thomas Banks and Hien T Tran. Mathematical and experimental modeling of physical and biological processes. Chapman and Hall/CRC, 2009.

[10] George I Bell and Ernest C Anderson. Cell growth and division: I. a mathematical model with applications to cell volume distributions in mammalian suspension cultures. Biophysical journal, 7(4):329, 1967.

[11] GI Bell and EC Anderson. Cell growth and division. iii. Conditions for balanced exponential growth in.

[12] Richard Bellman and Kenneth L Cooke. Asymptotic behavior of solutions of differential-difference equations, volume 35. American Mathematical Soc., 1959.

[13] Richard Bellman and Kenneth L Cooke. Stability theory and adjoint operators for linear differential-difference equations. Transactions of the American Mathematical Society, 92(3):470–500, 1959.

[14] Bielefeld. Carbon fixation, 2014.

[15] Felix E Browder. On the spectral theory of elliptic differential operators. i. Mathematische Annalen, 142(1):22–130, 1961.

[16] Hermann Brunner. Volterra integral equations: an introduction to theory and applications, volume 30. Cambridge University Press, 2017.

[17] Jeffrey C Cameron, Steven C Wilson, Susan L Bernstein, and Cheryl A Kerfeld. Biogenesis of a bacterial organelle: the carboxysome assembly pathway. Cell, 155(5):1131–1140, 2013.

[18] Manuel Campos, Ivan V Surovtsev, Setsu Kato, Ahmad Paintdakhi, Bruno Beltran, Sarah E Ebmeier, and Christine Jacobs-Wagner. A constant size extension drives bacterial cell size homeostasis. Cell, 159(6):1433–1446, 2014.

[19] Carlos Castillo-Chavez and Zhilan Feng. Global stability of an age-structure model for tb and its applications to optimal vaccination strategies. Mathematical biosciences, 151(2):135–154, 1998.

[20] Ryan L Clark, Jeffrey C Cameron, Thatcher W Root, and Brian F Pfleger. Insights into the industrial growth of cyanobacteria from a model of the carbon-concentrating mechanism. AIChE Journal, 60(4):1269–1277, 2014.

[21] Ph Clément, O Diekmann, M Gyllenberg, HJAM Heijmans, and HR Thieme. Perturbation theory for dual semigroups. Mathematische Annalen, 277(4):709–725, 1987.

[22] Ph Clément, O Diekmann, M Gyllenberg, HJAM Heijmans, and HR Thieme. A hille-yosida theorem for a class of weakly continuous semigroups. In Semigroup Forum, volume 38, pages 157–178. Springer, 1989.

[23] Odo Diekmann. Perturbed dual semigroups and delay equations. In Dynamics of infinite dimensional systems, pages 67–73. Springer, 1987.

[24] Odo Diekmann. On semigroups. and populations. 1989.

[25] Odo Diekmann and Mats Gyllenberg. Abstract delay equations inspired by population dynamics. In Functional analysis and evolution equations, pages 187–200. Springer, 2007.

[26] Odo Diekmann, Mats Gyllenberg, and Henk JAM Heijmans. When Are Two C0 Semigroups Related by a Bounded Perturbation? CRC Press, 2020.

[27] Odo Diekmann, Mats Gyllenberg, Haiyang Huang, Markus Kirkilionis, JAJ Metz, and Horst R Thieme. On the formulation and analysis of general deterministic structured population models ii. nonlinear theory. Journal of mathematical biology, 43(2):157–189, 2001.

[28] Odo Diekmann, Mats Gyllenberg, JAJ Metz, and Horst R Thieme. On the formulation and analysis of general deterministic structured population models i. linear theory. Journal of Mathematical Biology, 36(4):349–388, 1998.

[29] Odo Diekmann, Mats Gyllenberg, and Johan Metz. Physiologically structured population models: towards a general mathematical theory. In Mathematics for ecology and environmental sciences, pages 5–20. Springer, 2007.

[30] Odo Diekmann, Mats Gyllenberg, and Horst R Thieme. Perturbing semigroups by solving stieltjes renewal equations. Differential and integral equations, 6(1):155–181, 1993.

[31] Klaus-Jochen Engel and Rainer Nagel. One-parameter semigroups for linear evolution equations. In Semigroup Forum, volume 63, pages 278–280. Springer, 2001.

[32] Klaus-Jochen Engel and Rainer Nagel. A short course on operator semigroups. Springer Science & Business Media, 2006.

[33] Jozsef Z Farkas. Note on asynchronous exponential growth for structured population models. Nonlinear analysis, theory, methods & applications, 67(2):618–622, 2007.

[34] William Feller. On the integral equation of renewal theory. In Selected Papers I, pages 567–591. Springer, 2015.

[35] Zhilan Feng, Wenzhang Huang, and Carlos Castillo-Chavez. Global behavior of a multi-group sis epidemic model with age structure. Journal of Differential Equations, 218(2):292–324, 2005.

[36] Luca Giomi, Zhihong You, Daniel Pearce, and Anupam Sengupta. Geometry and mechanics of micro-domains in growing bacterial colonies. In APS March Meeting Abstracts, volume 2018, pages V53–013, 2018.

[37] C Raul Gonzalez-Esquer, Sarah E Newnham, and Cheryl A Kerfeld. Bacterial microcompartments as metabolic modules for plant synthetic biology. The Plant Journal, 87(1):66–75, 2016.

[38] Günther Greiner and Rainer Nagel. Growth of cell populations via one-parameter semigroups of positive operators. In Mathematics applied to science, pages 79–105. Elsevier, 1988.

[39] Morton E Gurtin and Richard C MacCamy. Non-linear age-dependent population dynamics. Archive for Rational Mechanics and Analysis, 54(3):281–300, 1974.

[40] Henk JAM Heijmans and Johan AJ Metz. Small parameters in structured population models and the trotter–kato theorem. SIAM Journal on Mathematical Analysis, 20(4):870–885, 1989.

[41] Nicholas C Hill, Jian Wei Tay, Sabina Altus, David M Bortz, and Jeffrey C Cameron. Life cycle of a cyanobacterial carboxysome. Science Advances, 6(19):eaba1269, 2020.

[42] John K Hunter and Bruno Nachtergaele. Applied analysis. World Scientific Publishing Company, 2001.

[43] Hisashi Inaba. A semigroup approach to the strong ergodic theorem of the multistate stable population process. Mathematical Population Studies, 1(1):49–77, 1988.

[44] Meri Lisi and Silvia Totaro. The chapman–enskog procedure for an age-structured population model: initial, boundary and corner layer corrections. Mathematical biosciences, 196(2):153–186, 2005.

[45] Benedict M Long, Wei Yih Hee, Robert E Sharwood, Benjamin D Rae, Sarah Kaines, Yi-Leen Lim, Nghiem D Nguyen, Baxter Massey, Soumi Bala, Susanne von Caemmerer, et al. Carboxysome encapsulation of the co 2-fixing enzyme rubisco in tobacco chloroplasts. Nature communications, 9(1):3570, 2018.

[46] Michael T Madigan, John M Martinko, Paul V Dunlap, and David P Clark. Brock biology of microorganisms 12th edn. Int. Microbiol, 11:65–73, 2008.

[47] Johan A Metz and Odo Diekmann. The dynamics of physiologically structured populations, volume 68. Springer, 2014.

[48] AG M'Kendrick. Applications of mathematics to medical problems. Proceedings of the Edinburgh Mathematical Society, 44:98–130, 1925.

[49] Kristin A Moore, Sabina Altus, Jian W Tay, Janet B Meehl, Evan B Johnson, David M Bortz, and Jeffrey C Cameron. Mechanical regulation of photosynthesis in cyanobacteria. Nature microbiology, 5(5):757–767, 2020.

[50] John T Nardini and David M Bortz. Investigation of a structured fisher's equation with applications in biochemistry. SIAM journal on applied mathematics, 78(3):1712–1736, 2018.

[51] Werner R Neumann and A Lorenzi. Evolution equations semigroups and functional analysis, 2002.

[52] Amnon Pazy. Semigroups of linear operators and applications to partial differential equations, volume 44. Springer Science & Business Media, 2012.

[53] Ian L Pepper, Charles P Gerba, Terry J Gentry, and Raina M Maier. Environmental microbiology. Academic press, 2011.

[54] Lawrence Perko. Differential equations and dynamical systems, volume 7. Springer Science & Business Media, 2013.

[55] Jan Prüß. Equilibrium solutions of age-specific population dynamics of several species. Journal of Mathematical Biology, 11(1):65–84, 1981.

[56] Eva Sánchez, Ovide Arino, Pierre Auger, and Rafael Bravo de la Parra. A singular perturbation in an age-structured population model. SIAM Journal on Applied Mathematics, 60(2):408–436, 2000.

[57] Bettina E Schirrmeister, Patricia Sanchez-Baracaldo, and David Wacey. Cyanobacterial evolution during the precambrian. International Journal of Astrobiology, 15(3):187–204, 2016.

[58] Francis R Sharpe and Alfred J Lotka. L. a problem in age-distribution. The London, Edinburgh, and Dublin Philosophical Magazine and Journal of Science, 21(124):435–438, 1911.

[59] James W Sinko and William Streifer. A new model for age-size structure of a population. Ecology, 48(6):910–918, 1967.

[60] Pin-Tzu Su, Chih-Tang Liao, Jiunn-Ren Roan, Shao-Hung Wang, Arthur Chiou, and Wan-Jr Syu. Bacterial colony from two-dimensional division to three-dimensional development. PloS one, 7(11):e48098, 2012.

[61] Horst R Thieme. Balanced exponential growth of operator semigroups. Journal of mathematical analysis and applications, 223(1):30–49, 1998.

[62] Horst R Thieme. Positive perturbation of operator semigroups: growth bounds, essential compactness and asynchronous exponential growth. Discrete & Continuous Dynamical Systems, 4(4):735, 1998.

[63] Susan L Tucker and Stuart O Zimmerman. A nonlinear model of population dynamics containing an arbitrary number of continuous structure variables. SIAM Journal on Applied Mathematics, 48(3):549–591, 1988.

[64] Jan Van Neerven. The asymptotic behaviour of semigroups of linear operators, volume 88. Birkhäuser, 2012.

[65] GF Webb. An operator-theoretic formulation of asynchronous exponential growth. Transactions of the American Mathematical Society, 303(2):751–763, 1987.

[66] GF Webb. Population models structured by age, size, and spatial position. In Structured population models in biology and epidemiology, pages 1–49. Springer, 2008.

[67] Glenn F Webb et al. Theory of nonlinear age-dependent population dynamics. CRC Press, 1985.

[68] S Zimmerman and RA White. Generalizations of a fluid dynamic model for analyzing multiparameter flow cytometric data. Biomathematics and Cell Kinetics, pages 403–409, 1981.

Appendix A

Proof of Jacobian and Exponential Term Equivalence

After integrating the PDE (3.4) along characteristic curves, we are are left with the exponential term

$$\exp\left[-\int_0^s \sum_{i=1}^{k} \frac{\partial v_i}{\partial X_i} d\sigma\right],$$

which we claim is equal to the Jacobian determinant,

$$\mathcal{J}(s) = \exp\left[-\int_0^s \sum_{i=1}^{k} \frac{\partial v_i}{\partial X_i} d\sigma\right] = \left|\frac{\partial(A(s,a), \bar{\mathbf{x}}(s,\bar{\mathbf{x}}))}{\partial(a,\bar{\mathbf{x}})}\right|.$$

The following is a proof of this claim using Liouville's Formula.

Liouville's Formula.
Consider the first-order, linear, homogeneous ODE

$$\frac{d\mathbf{r}}{dt} = K(t)\mathbf{r}(t), \quad \mathbf{r}(0) = \mathbf{r}_0, \quad \mathbf{r} \in \mathbb{R}^n$$

with fundamental matrix solution $\mathbf{\Phi}(t)$ satisfying

$$\mathbf{\Phi}'(t) = K(t)\mathbf{\Phi}(t), \quad \mathbf{\Phi}(0) = I.$$

The determinant of $\mathbf{\Phi}(x)$ then satisfies the ODE,

$$\frac{d}{dt}\det(\mathbf{\Phi}(t)) = Tr(K(t))\det(\mathbf{\Phi}(t)),$$

with solution,

$$\det(\mathbf{\Phi}(t)) = \det(\mathbf{\Phi}(t_0))\exp\left[\int_{t_0}^{t} Tr(K(s))ds\right]$$

where $Tr(K)$ is the trace of K, the sum of its diagonal elements.

To make the extension to the arbitrary k-dimensional model clear, first assume that $k = 2$ and let $x_1 = x$, $x_2 = y$, $\frac{dx}{dt} = g(a, x, y)$, and $\frac{dy}{dt} = f(a, x, y)$, so that our population distribution is given by $n(t, a, x, y)$.

This gives the following system of ODEs and solutions,

$$\begin{cases} \frac{da}{dt} = 1, & A(t,a) = a - t \\ \frac{dx}{dt} = g(a,x,y), & X(t,x) = G^{-1}(G(x) - t), \quad G(x) = \int_{x_m}^{x} \frac{1}{g(a,s,y)} ds \\ \frac{dy}{dt} = f(a,x,y), & Y(t,y) = F^{-1}(F(y) - t), \quad F(y) = \int_{y_m}^{y} \frac{1}{f(a,x,s)} ds. \end{cases}$$

Capital letters again denote *solutions* to this system of ODEs, i.e., characteristic curves. $\mathbf{X} = (A, X, Y)^T$ are all functions of t, but $\mathbf{x} = (a, x, y)^T$ are not. Denote by $\mathbf{v}$ the vector field $(1, g, f)$. Lastly, note that $A(0, a) = a, X(0, x) = x$, and $Y(0, y) = y$.

The matrix $K(t)$ from Liouville's Formula is $D_{\mathbf{X}}\mathbf{v}(t, \mathbf{X})$:

$$K(t) = \begin{bmatrix} \frac{\partial(1)}{\partial A} & \frac{\partial(1)}{\partial X} & \frac{\partial(1)}{\partial Y} \\ \frac{\partial g}{\partial A} & \frac{\partial g}{\partial X} & \frac{\partial g}{\partial Y} \\ \frac{\partial f}{\partial A} & \frac{\partial f}{\partial X} & \frac{\partial f}{\partial Y} \end{bmatrix}_{(A,X,Y)} = \begin{bmatrix} 0 & 0 & 0 \\ \frac{\partial g}{\partial A} & \frac{\partial g}{\partial X} & \frac{\partial g}{\partial Y} \\ \frac{\partial f}{\partial A} & \frac{\partial f}{\partial X} & \frac{\partial f}{\partial Y} \end{bmatrix}_{(A,X,Y)}$$

and the trace of $K(t)$ is $\frac{\partial g}{\partial X} + \frac{\partial f}{\partial Y} = \nabla \cdot \mathbf{v}$, the divergence of $\mathbf{v}$.

The fundamental solution $\mathbf{\Phi}(t)$ for the system $\mathbf{\Phi}'(t) = K(t)\mathbf{\Phi}(t)$ is $D_{\mathbf{x}}\mathbf{X}(t, \mathbf{x})$, the Jacobian matrix of the characteristic curves:

$$\mathbf{\Phi}(t) = \begin{bmatrix} \frac{\partial A}{\partial a} & \frac{\partial A}{\partial x} & \frac{\partial A}{\partial y} \\ \frac{\partial X}{\partial a} & \frac{\partial X}{\partial x} & \frac{\partial X}{\partial y} \\ \frac{\partial Y}{\partial a} & \frac{\partial Y}{\partial x} & \frac{\partial Y}{\partial y} \end{bmatrix} = \begin{bmatrix} 1 & 0 & 0 \\ 0 & \frac{g(a,X,y)}{g(a,x,y)} & 0 \\ 0 & 0 & \frac{f(a,x,Y)}{f(a,x,y)} \end{bmatrix}$$

which is equal to the identity matrix I when evaluated at $t = 0$.

Note: To be clear, the off-diagonal entries such as, $\frac{\partial X}{\partial a}$, are, in fact, zero. When we write $G(x) = \int_{x_m}^{x} \frac{1}{g(a,s,y)} ds$, this is purely a function of x as a and y are understood to be fixed. Therefore, differentiating X with respect to a or y is zero, and not $g(a, X, y) \int_0^x -\frac{\frac{\partial g}{\partial a}(a,s,y)}{(g(a,s,y))^2}$, what you would get if $G(x)$ were $G(a, x, y)$.

The determinant of this matrix is, $\frac{g(a,X,y)}{g(a,x,y)} \cdot \frac{f(a,x,Y)}{f(a,x,y)}$, consistent with Liouville's Formula.

$$\begin{aligned}
\frac{d}{dt}\det(\mathbf{\Phi}(t)) &= \frac{d}{dt}\left[\frac{g(a,X,y)}{g(a,x,y)} \cdot \frac{f(a,x,Y)}{f(a,x,y)}\right] \\
&= \frac{-g(a,X,y)\frac{\partial g}{\partial x}(a,X,y)}{g(a,x,y)} \cdot \frac{f(a,x,Y)}{f(a,x,y)} - \frac{-f(a,x,Y)\frac{\partial f}{\partial y}(a,x,Y)}{f(a,x,y)} \cdot \frac{g(a,X,y)}{g(a,x,y)} \\
&= -\left(\frac{\partial g}{\partial x}(a,X,y) + \frac{\partial f}{\partial y}(a,x,Y)\right)\left(\frac{g(a,X,y)}{g(a,x,y)} \cdot \frac{f(a,x,Y)}{f(a,x,y)}\right) \\
&= -tr(K(t))\det(\mathbf{\Phi}(t))
\end{aligned}$$

Applying Liouville's formula, we see that

$$\det(\mathbf{\Phi}(t)) = \det(\mathbf{\Phi}(0))\exp\left[-\int_0^t Tr(K(s))ds\right] = \exp\left[-\int_0^t \nabla \cdot \mathbf{v}(A,X,Y)ds\right].$$

The extension to the arbitrary k case is tedious but straightforward, and thus not included.

■

Secondary Claim: $\mathcal{J}(s)$ is bounded.

Conditions imposed on the velocity functions v_i such as, boundedness, continuity, and regularity (see Section 1), are what make $\mathcal{J}$ bounded. On the interior of Ω, $v_i(a,X,y)/v_i(a,x,y)$ is bounded. The product of bounded functions is also bounded, and as a result, $\mathcal{J}(s)$ is always bounded, and we can say that $||\mathcal{J}(s)||_\infty = 1$. ■

Appendix B

Proof of Stability of the Zero Solution

Suppose that $\lambda \in \sigma(\mathcal{A}) \setminus \sigma_{ess}(\mathcal{A})$, the complement of the essential spectrum in the spectrum of $\mathcal{A}$. There is a result (from [15]) which states that because $\mathcal{A}$ is closed in $L^1(\mathbb{R}_+ \times \Omega)$, such a λ is an eigenvalue of $\mathcal{A}$. This means that there exists some $u(a, \bar{\mathbf{x}})$ such that $(\lambda I - \mathcal{A})u = 0$.

$$\begin{aligned}(\lambda I - \mathcal{A})u(a, \bar{\mathbf{x}}) &= \lambda u + \frac{\partial u}{\partial a} + \sum_{i=1}^{k} v_i \frac{\partial u}{\partial x_i} + u \sum_{i=1}^{k} \frac{\partial v_i}{\partial x_i} + \mu u \\ &= \frac{\partial u}{\partial a} + \sum_{i=1}^{k} v_i \frac{\partial u}{\partial x_i} + u \sum_{i=1}^{k} \frac{\partial v_i}{\partial x_i} + (\mu + \lambda)u \\ &= 0\end{aligned} \tag{B.1}$$

We solve this 'new' PDE using the method of characteristics as follows.

$$\frac{\partial u}{\partial a} + \sum_{i=1}^{k} v_i \frac{\partial u}{\partial x_i} = -\left[\nabla \cdot \bar{\mathbf{v}} + (\mu + \lambda)\right] u \tag{B.2}$$

$$\frac{da}{d\theta} = 1, \quad a(0) = 0 \qquad \Rightarrow \boxed{a = \theta}$$

$$\frac{dx_i}{da} = v_i(a, \bar{\mathbf{x}}), \quad x_i(0) = \tilde{x}_i \qquad \Rightarrow G(x_i) - G(\tilde{x}_i) = a + c$$

$$c = 0 \Rightarrow \boxed{\tilde{x}_i = G^{-1}(G(x_i) - a)}$$

$$\frac{du}{da} = -\left(\mu(a, \bar{\mathbf{x}}) + \lambda + \nabla \cdot \bar{\mathbf{v}}\right) u(a, \bar{\mathbf{x}}) \qquad \Rightarrow u(a, \bar{\mathbf{x}}) = c e^{-\int_0^a (\mu + \lambda + \nabla \cdot \bar{\mathbf{v}}) da'} \tag{B.3}$$

Now use an initial/boundary condition to solve for c.

The first condition of the domain of $\mathcal{A}$ says that,

$$\lim_{t\to 0^+} \frac{1}{t}\int_0^t \int_\Omega |u(a,\bar{\mathbf{x}}) - \hat{B}(0,\bar{\mathbf{x}})| d\bar{\mathbf{x}} da = 0.$$

Using l'Hopital's rule, we can write this limit as,

$$\begin{aligned}\lim_{t\to 0^+} \frac{\frac{d}{dt}\int_0^t \int_\Omega |u(a,\bar{\mathbf{x}}) - \hat{B}(0,\bar{\mathbf{x}})| d\bar{\mathbf{x}} da}{\frac{d}{dt}t} &= \lim_{t\to 0^+} \frac{\int_\Omega |u(t,\bar{\mathbf{x}}) - \hat{B}(0,\bar{\mathbf{x}})| d\bar{\mathbf{x}}}{1} \\ &= \int_\Omega |u(0,\bar{\mathbf{x}}) - \hat{B}(0,\bar{\mathbf{x}})| d\bar{\mathbf{x}} = 0.\end{aligned}$$

This implies that the integrand, $|u(0,\bar{\mathbf{x}}) - \hat{B}(0,\bar{\mathbf{x}})| = 0$, and therefore

$$u(0,\bar{\mathbf{x}}) = c = \hat{B}(0,\bar{\mathbf{x}}) = \int_0^\infty \int_\Omega \beta(a,\bar{\mathbf{y}},\bar{\mathbf{x}}) S(0) u(a,\bar{\mathbf{y}}) d\bar{\mathbf{y}} da = \int_0^\infty \int_\Omega \beta(a,\bar{\mathbf{y}},\bar{\mathbf{x}}) u(a,\bar{\mathbf{y}}) d\bar{\mathbf{y}} da.$$

Returning to our solution for u, we get:

$$\begin{aligned}u(a,\bar{\mathbf{x}}) &= \int_0^\infty \int_\Omega \beta(a,\bar{\mathbf{y}},\bar{\mathbf{x}}) u(a,\bar{\mathbf{y}}) d\bar{\mathbf{y}} da \cdot \exp\left[-\int_0^a (\mu + \lambda + \nabla\cdot\bar{\mathbf{v}})\, da'\right] \\ &= \int_0^\infty \int_\Omega \beta(a,\bar{\mathbf{y}},\bar{\mathbf{x}}) u(a,\bar{\mathbf{y}}) d\bar{\mathbf{y}} da \cdot \exp\left[-\int_0^a \left(\mu(a',\bar{\mathbf{G}}^{-1}(\bar{\mathbf{G}}(\bar{\mathbf{x}}) - a')) + \lambda\right) da'\right] \mathcal{J}(a)\end{aligned} \tag{B.4}$$

Which we can bound by:

$$\begin{aligned}||u(a,\bar{\mathbf{x}})||_1 &= \int_0^\infty \int_\Omega \left| \int_0^\infty \int_\Omega \beta(a,\bar{\mathbf{y}},\bar{\mathbf{x}}) u(a,\bar{\mathbf{y}}) d\bar{\mathbf{y}} da \cdot \exp\left[-\int_0^a (\mu+\lambda)\, da'\right] \mathcal{J}(a)\right| d\bar{\mathbf{x}} da \\ &\le \bar{\beta}\mathcal{V}_\Omega ||u||_1 \int_0^\infty \exp\left[-\int_0^a (\mu + Re(\lambda))\, da'\right] da \\ &= \bar{\beta}\mathcal{V}_\Omega ||u||_1 \cdot \left.\frac{\exp\left[-\int_0^a (\mu+Re(\lambda))\, da'\right]}{-(Re(\lambda)+\mu(a,\bar{\mathbf{x}}))}\right|_0^\infty \\ \Rightarrow ||u(a,\bar{\mathbf{x}})||_1 &\le \frac{\bar{\beta}\mathcal{V}_\Omega ||u(a,\bar{\mathbf{x}})||_1}{Re(\lambda)+\mu(a,\bar{\mathbf{x}})}\end{aligned}$$

where $\bar{\beta}$ is an upper bound on the birth modulus β, and $\mathcal{V}_\Omega = \int_\Omega d\bar{\mathbf{x}}$ is the volume of Ω.

Provided $\mu(a,\bar{\mathbf{x}}) > -Re(\lambda)$,

$$Re(\lambda) \le \bar{\beta}\mathcal{V}_\Omega - \mu(a,\bar{\mathbf{x}}).$$

We can guarantee that $\sup_{\lambda\in\sigma(\mathcal{A})\setminus\sigma_{ess}(\mathcal{A})}\{Re(\lambda)\}$ is negative as long as μ is sufficiently large, i.e. $\mu > \max\{\bar{\beta}\mathcal{V}_\Omega, -Re(\lambda)\}$.

There is a theorem (cited in [63]) that states that if

$$\sup_{\lambda\in\sigma(\mathcal{A})\setminus\sigma_{ess}(\mathcal{A})}\{Re(\lambda)\} < 0,$$

then the solution u is locally asymptotically stable. ■

That is, for every initial population relatively close to zero, the solution will tend to zero as $t \to \infty$. Moreover, this should imply that we will have a nonzero population whenever $\mu(a, \bar{\mathbf{x}})$ is not large enough that $\sup_{\lambda\in\sigma(\mathcal{A})\setminus\sigma_{ess}(\mathcal{A})}\{Re(\lambda)\} \geq 0$.

Appendix C

Definitions for the Spectrum of Linear Operators

These definitions are collected from [42] and [4].

Let L be a closed and bounded linear operator with domain $\mathcal{D}(L)$ dense in a Banach space B.

Definition 1. The *resolvent set* of L, denoted $\rho(L)$, is the open set

$$\rho(L) = \{\lambda \in \mathbb{C} : (L - \lambda I) \text{ is one-to-one and onto}\}.$$

The Open Mapping Theorem [42] implies that $(L - \lambda I)^{-1}$ is bounded for $\lambda \in \rho(L)$.

Definition 2. The *resolvent operator*, denoted by $R(\lambda, L)$ or R_λ, is the operator-valued function

$$(L - \lambda I)^{-1}$$

defined only on the set $\rho(L)$.

Definition 3. The *spectrum* of L, denoted $\sigma(L)$, is the closed set

$$\sigma(L) = \mathbb{C} \setminus \rho(L) = \{\lambda \in \mathbb{C} : (L - \lambda I) \text{ is not boundedly invertible}\}.$$

The spectrum is composed of three disjoint sets:

$$\sigma(L) = \sigma_P(L) \cup \sigma_C(L) \cup \sigma_R(L)$$

- The *point spectrum*

$$\sigma_P(L) = \{\lambda \in \sigma(L) : (L - \lambda I) \text{ is not one-to-one}\}.$$

These are the eigenvalues of L.

- The *continuous spectrum*

$$\sigma_C(L) = \{\lambda \in \sigma(L) : (L - \lambda I) \text{ is one-to-one but not onto,} \\ \text{and the range of } (L - \lambda I) \text{ is dense in } B\}.$$

- The *residual spectrum*

$$\sigma_R(L) = \{\lambda \in \sigma(L) : (L - \lambda I) \text{ is one-to-one but not onto,} \\ \text{and the range of } (L - \lambda I) \text{ is not dense in } B\}.$$

Definition 4. The *spectral radius*, denoted $r(L)$, is a bound on $\sigma(L)$—the radius of smallest disk centered at zero containing $\sigma(L)$,

$$r(L) = \sup\{|\lambda| : \lambda \in \sigma(L)\}.$$

Note that if N is a nilpotent operator, i.e., $\exists m : N^m = 0$, $\sigma(N) = \{0\}$ and therefore, $r(N) = 0$. The spectral radius can be thought of as a measure of the distance from L to the set of nilpotent operators, and this is reflected in the formula

$$r(L) = \lim_{m \to \infty} ||L^m||^{1/m}.$$

Definition 5. The essential spectrum, denoted $\sigma_{ess}(L)$, is the set of $\lambda \in \sigma(L)$ such that at least one of the following holds:

(1) The range of $(L - \lambda I)$ is not closed.

(2) The generalized eigenspace associated with $(L - \lambda I)$ is infinite dimensional.

(3) λ is a limit point of $\sigma(L)$.

Appendix D

Proof of Semigroup Properties

$S(t)$ satisfies the four defining properties of a strongly continuous semigroup.

(1) $S(t)$ is a continuous mapping.

Let $\varepsilon > 0$ and $||\phi(a, \bar{\mathbf{x}}) - \phi(b, \bar{\mathbf{y}})|| < \varepsilon$ where $||\cdot||$ is the L^1-norm. We require that ϕ be continuously differentiable.

Then,

$$
\begin{aligned}
&||(S(t)\phi)(a, \bar{\mathbf{x}}) - (S(t)\phi)(b, \bar{\mathbf{y}})|| \\
&\quad = ||\phi(a-t, \bar{\mathbf{G}}^{-1}(\bar{\mathbf{G}}(\bar{\mathbf{x}}) - t))\mathcal{P}(t,-t)\mathcal{J}(t) \\
&\quad - \phi(b-t, \bar{\mathbf{G}}^{-1}(\bar{\mathbf{G}}(\bar{\mathbf{y}}) - t))\mathcal{P}(t,-t)\mathcal{J}(t)|| \\
&\quad = ||[\phi(a-t, \bar{\mathbf{G}}^{-1}(\bar{\mathbf{G}}(\bar{\mathbf{x}}) - t)) - \phi(b-t, \bar{\mathbf{G}}^{-1}(\bar{\mathbf{G}}(\bar{\mathbf{y}}) - t))]\mathcal{P}(t,-t)\mathcal{J}(t)|| \\
&\quad \leq ||\phi(a-t, \bar{\mathbf{G}}^{-1}(\bar{\mathbf{G}}(\bar{\mathbf{x}}) - t)) - \phi(b-t, \bar{\mathbf{G}}^{-1}(\bar{\mathbf{G}}(\bar{\mathbf{y}}) - t))|| \\
&\quad \cdot ||\mathcal{P}(t,-t)||_\infty \cdot ||\mathcal{J}(t)||_\infty \\
&\quad = ||\mathcal{J}(t)||_\infty ||\phi(a-t, \bar{\mathbf{G}}^{-1}(\bar{\mathbf{G}}(\bar{\mathbf{x}}) - t)) \\
&\quad - \phi(b-t, \bar{\mathbf{G}}^{-1}(\bar{\mathbf{G}}(\bar{\mathbf{y}}) - t))||
\end{aligned}
$$

Consider only the difference in ϕ for now. We will show that this difference is bounded in the age-and-size-structured case where $\phi(a, \bar{\mathbf{x}})$ becomes $\phi(a, x)$, a function of age and size only, with the growth rate g for v_1. The following arguments can be extended naturally to the multi-structured model.

$$
\begin{aligned}
&||\phi(a-t, G^{-1}(G(x-t)) - \phi(b-t, G^{-1}(G(y)-t))|| \\
&\quad = \left|\left|\phi(a,x) - t\left(\frac{1}{G'(x)}\frac{\partial\phi}{\partial x}(a,x) + \frac{\partial\phi}{\partial a}(a,x)\right)\right.\right. \\
&\quad \left.\left. - \left[\phi(b,y) - t\left(\frac{1}{G'(y)}\frac{\partial\phi}{\partial y}(b,y) + \frac{\partial\phi}{\partial b}(b,x)\right)\right]\right|\right| \\
&\quad = \left|\left|\phi(a,x) - t\left(g(a,x)\frac{\partial\phi}{\partial x}(a,x) + \frac{\partial\phi}{\partial a}(a,x)\right)\right.\right. \\
&\quad \left.\left. - \left[\phi(b,y) - t\left(g(b,y)\frac{\partial\phi}{\partial y}(b,y) + \frac{\partial\phi}{\partial b}(b,y)\right)\right]\right|\right| \\
&\quad \leq ||\phi(a,x) - \phi(b,y)|| + \left|\left|t\left[g(b,y)\frac{\partial\phi}{\partial y}(b,y) + \frac{\partial\phi}{\partial b}(b,y)\right.\right.\right. \\
&\quad \left.\left.\left. - \left(g(a,x)\frac{\partial\phi}{\partial x}(a,x) + \frac{\partial\phi}{\partial a}(a,x)\right)\right]\right|\right| \\
&\quad \leq \varepsilon + \left|\left|t\left(g(b,y)\frac{\partial\phi}{\partial y}(b,y) - g(a,x)\frac{\partial\phi}{\partial x}(a,x)\right)\right|\right| \\
&\quad + \left|\left|t\left(\frac{\partial\phi}{\partial b}(b,y) - \frac{\partial\phi}{\partial a}(a,x)\right)\right|\right| \\
&\quad = \varepsilon + \left|\left|t\left(g(b,y)\frac{\partial\phi}{\partial y}(b,y) - g(a,x)\frac{\partial\phi}{\partial x}(a,x)\right)\right|\right| + |t|\varepsilon_3 \\
&\quad = \varepsilon + \left|\left|t\left(g(b,y)\frac{\partial\phi}{\partial y}(b,y) - g(a,x)\frac{\partial\phi}{\partial x}(a,x)\right)\right|\right| + |t|\varepsilon_3 \\
&\quad = \varepsilon + |t|\left|\left|g(b,y)\frac{\partial\phi}{\partial y}(b,y) - g(b,y)\frac{\partial\phi}{\partial x}(a,x)\right.\right. \\
&\quad \left.\left. + g(b,y)\frac{\partial\phi}{\partial x}(a,x) - g(a,x)\frac{\partial\phi}{\partial x}(a,x)\right|\right| + |t|\varepsilon_3 \\
&\quad = \varepsilon + |t|\left|\left|g(b,y)\left(\frac{\partial\phi}{\partial y}(b,y) - \frac{\partial\phi}{\partial x}(a,x)\right)\right.\right. \\
&\quad \left.\left. + \frac{\partial\phi}{\partial x}(a,x)\left(g(b,y) - g(a,x)\right)\right|\right| + |t|\varepsilon_3
\end{aligned}
$$

$$
\begin{aligned}
&\leq \varepsilon + |t| \left|\left| g(b,y) \left(\frac{\partial \phi}{\partial y}(b,y) - \frac{\partial \phi}{\partial x}(a,x) \right) \right|\right| \\
&+ |t| \left|\left| \frac{\partial \phi}{\partial x}(a,x) \left(g(b,y) - g(a,x) \right) \right|\right| + |t|\varepsilon_3 \\
&\leq \varepsilon + |t| \left(||g(b,y)||_\infty \left|\left| \frac{\partial \phi}{\partial y}(b,y) - \frac{\partial \phi}{\partial x}(a,x) \right|\right| \right. \\
&\left. + \left|\left| \frac{\partial \phi}{\partial x}(a,x) \right|\right|_\infty \left|\left| g(b,y) - g(a,x) \right|\right| \right) + |t|\varepsilon_3 \\
&\leq \varepsilon + |t| \left(\varepsilon_a ||g(b,y)||_\infty + \varepsilon_b \left|\left| \frac{\partial \phi}{\partial x}(a,x) \right|\right|_\infty \right) + |t|\varepsilon_3 \\
&= \varepsilon + |t|(\varepsilon_2 + \varepsilon_3)
\end{aligned}
$$

where $\varepsilon_a = \varepsilon_2/2||g||_\infty$, $\varepsilon_b = \varepsilon_2/2||\partial\phi/\partial x||_\infty$, and ε_3 comes from the fact that ϕ must be continuously differentiable. (You could also get ε_2 from the fact that the product of continuous functions are is continuous.)

Finally,

$$||(S(t)\phi)(a,x) - (S(t)\phi)(b,y)|| \leq \varepsilon + |t|(\varepsilon_2 + \varepsilon_3) = \delta(\varepsilon).$$

Since for every ε such that $||\phi(a,x) - \phi(b,y)|| < \varepsilon$ there exists a $\delta(\varepsilon) > 0$ such that $||(S(t)\phi)(a,x) - (S(t)\phi)(b,y)|| \leq \delta$, the mapping is continuous.

(2) $S(0) = I$.

$$
\begin{aligned}
(S(0)\phi)(a,\bar{\mathbf{x}}) &= \phi(a-0, \bar{\mathbf{G}}^{-1}(\bar{\mathbf{G}}(\bar{\mathbf{x}}) - 0))\mathcal{J}(0) \\
&\quad \times \exp\left[- \int_0^0 \mu(a-t', \bar{\mathbf{G}}^{-1}(\bar{\mathbf{G}}(\bar{\mathbf{x}}) - t'))dt' \right] \\
&= \phi(a,\bar{\mathbf{x}}) = (I\phi)(\bar{\mathbf{x}}) \\
&\Rightarrow S(0) = I
\end{aligned}
$$

(3) The semigroup property: $S(s)S(t)\phi = S(t+s)\phi$.

$$\begin{aligned}
S(s)[(S(t)\phi)](a,x) &= (S(s)\phi)(a-t, \bar{\mathbf{G}}^{-1}(\bar{\mathbf{G}}(\bar{\mathbf{x}})-t))\mathcal{P}(t,-t)\mathcal{J}(t) \\
&= \phi((a-t)-s, \bar{\mathbf{G}}^{-1}((\bar{\mathbf{G}}(\bar{\mathbf{x}})-t)-s))\mathcal{P}(t,-t) \\
&\times e^{\left[-\int_t^s \mu(a-t', \bar{\mathbf{G}}^{-1}(\bar{\mathbf{G}}(\bar{\mathbf{x}})-t'))dt'\right]}\mathcal{J}(t)e^{\int_t^s \nabla\cdot\bar{\mathbf{v}}dt'} \\
&= \phi(a-(t+s), \bar{\mathbf{G}}^{-1}(\bar{\mathbf{G}}(\bar{\mathbf{x}})-(t+s))\mathcal{P}(t+s,-t)\mathcal{J}(t+s) \\
&= (S(t+s)\phi)(a,\bar{\mathbf{x}})
\end{aligned}$$

Where

$$\begin{aligned}
\mathcal{P}(t,-t)e^{\left[-\int_t^s \mu(a-t', \bar{\mathbf{G}}^{-1}(\bar{\mathbf{G}}(\bar{\mathbf{x}})-t'))dt'\right]} &= e^{\left[-\int_0^t \mu(a-t', \bar{\mathbf{G}}^{-1}(\bar{\mathbf{G}}(\bar{\mathbf{x}})-t'))dt'\right]} \\
&\times e^{\left[-\int_t^s \mu(a-s', \bar{\mathbf{G}}^{-1}(\bar{\mathbf{G}}(\bar{\mathbf{x}})-s'))ds'\right]} \\
&= \exp\left[-\left(\int_0^t \mu dt' + \int_t^s \mu dt'\right)\right] \\
&= \exp\left[-\int_0^{t+s} \mu(a-t', \bar{\mathbf{G}}^{-1}(\bar{\mathbf{G}}(\bar{\mathbf{x}})-t'))dt'\right] \\
&= \mathcal{P}(t+s,-t)
\end{aligned}$$

and similarly for $\mathcal{J}(t+s)$.

(4) Strong continuity: $\lim_{t\searrow 0}||S(t)\phi - \phi|| = 0$ where $||\cdot||$ is the operator norm in the Banach space $B = L^1$.

$$\begin{aligned}
\lim_{t\searrow 0}||S(t)\phi - \phi|| &= \lim_{t\searrow 0}||\phi(a-t, \bar{\mathbf{G}}^{-1}(\bar{\mathbf{G}}(\bar{\mathbf{x}})-t))\mathcal{P}(t,-t)\mathcal{J}(t) - \phi(a,x)|| \\
&= ||\lim_{t\searrow 0}\phi(a-t, \bar{\mathbf{G}}^{-1}(\bar{\mathbf{G}}(\bar{\mathbf{x}})-t))\mathcal{P}(t,-t)\mathcal{J}(t) - \phi(a,\bar{\mathbf{x}})|| \\
&= 0
\end{aligned}$$

Therefore, $\{S(t)\}_{t\geq 0}$ forms a strongly continuous semigroup on $L^1(\mathbb{R}_+ \times \Omega)$. ■

Appendix E

Infinitesimal Generator Proof

Proof that $\mathcal{A}$ is the infinitesimal generator of the strongly-continuous semigroup $S(t)$

An operator $\mathcal{A}$ is the generator of a semigroup if

$$\mathcal{A}\phi = \lim_{t \searrow 0} \frac{1}{t}(S(t)\phi - \phi)$$

for every $\phi \in \mathcal{D}(\mathcal{A})$.

$$\begin{aligned}\lim_{t \searrow 0} \frac{1}{t}\left(S(t)\phi - \phi\right) &= \lim_{t \searrow 0} \frac{1}{t}\left(\phi(a-t, \bar{\mathbf{G}}^{-1}(\bar{\mathbf{G}}(\bar{\mathbf{x}}) - t))\mathcal{P}(t,-t)\mathcal{J}(t) - \phi(a, \bar{\mathbf{x}})\right) \\ &= \lim_{t \searrow 0} \frac{1}{t}\Bigg(\phi(a-t, \bar{\mathbf{G}}^{-1}(\bar{\mathbf{G}}(\bar{\mathbf{x}}) - t)) \exp\left[-\int_0^t \mu(a-t', \bar{\mathbf{G}}^{-1}(\bar{\mathbf{G}}(\bar{\mathbf{x}}) - t'))dt'\right] \\ &\quad \cdot \exp\left[-\int_0^t \nabla \cdot \bar{\mathbf{v}}(a-t, \bar{\mathbf{G}}^{-1}(\bar{\mathbf{G}}(\bar{\mathbf{x}}) - t'))dt'\right] - \phi(a, \bar{\mathbf{x}})\Bigg)\end{aligned} \tag{E.1}$$

In the next step, we proceed by expanding each term in a Taylor series

about zero from the right.

$$
\begin{aligned}
=&\lim_{t\searrow 0}\frac{1}{t}\Big(\phi(a,\bar{\mathbf{x}})-t\Big[\frac{\partial\phi}{\partial a}(a,\bar{\mathbf{x}})+\sum_{i=1}^{k}v_i(a,\bar{\mathbf{x}})\frac{\partial\phi}{\partial x_i}(a,\bar{\mathbf{x}})+\phi(a,\bar{\mathbf{x}})\sum_{i=1}^{k}\frac{\partial v_i}{\partial x_i}(a,\bar{\mathbf{x}})\\
&+\mu(a,\bar{\mathbf{x}})\phi(a,\bar{\mathbf{x}})\Big]+\mathcal{O}(t^2)-\phi(a,\bar{\mathbf{x}})\Big)\\
=&\lim_{t\searrow 0}\Big(\frac{\partial\phi}{\partial a}(a,\bar{\mathbf{x}})+\sum_{i=1}^{k}v_i(a,\bar{\mathbf{x}})\frac{\partial\phi}{\partial x_i}(a,\bar{\mathbf{x}})+\phi(a,\bar{\mathbf{x}})\sum_{i=1}^{k}\frac{\partial v_i}{\partial x_i}(a,\bar{\mathbf{x}})\\
&+\mu(a,\bar{\mathbf{x}})\phi(a,\bar{\mathbf{x}})+\mathcal{O}(t)\Big)\\
=&-\Big(\frac{\partial\phi}{\partial a}(a,\bar{\mathbf{x}})+\sum_{i=1}^{k}v_i(a,\bar{\mathbf{x}})\frac{\partial\phi}{\partial x_i}(a,\bar{\mathbf{x}})+\phi(a,\bar{\mathbf{x}})\sum_{i=1}^{k}\frac{\partial v_i}{\partial x_i}(a,\bar{\mathbf{x}})\\
&+\mu(a,\bar{\mathbf{x}})\phi(a,\bar{\mathbf{x}})\Big)\\
=&-\left(\frac{\partial\phi}{\partial a}+\sum_{i=1}^{k}v_i\frac{\partial\phi}{\partial x_i}+\phi\sum_{i=1}^{k}\frac{\partial v_i}{\partial x_i}+\mu\phi\right)\\
=&\mathcal{A}\phi
\end{aligned}
\tag{E.2}
$$

Therefore, $\mathcal{A}$ is the infinitesimal generator of the strongly continuous one-parameter semigroup $\{S(t)\}_{t\geq 0}$. ■